

# **Application of Computer-Based Methods to Design Inhibitors of Zinc-Dependent Enzymes**

DISSERTATION

zur Erlangen des akademischen Grades

Doctor rerum naturalium (Dr. rer. nat.)

der Naturwissenschaftlichen Fakultät I Biowissenschaften

der Martin-Luther-Universität Halle-Wittenberg

von

**Jelena Melesina**

geboren am 20. April 1986

Gutachter:

1. Prof. Dr. Wolfgang Sippl, Halle
2. Prof. Dr. Mike Schutkowski, Halle
3. Prof. Dr. Gerhard Wolber, Berlin

Datum der Disputation: 16.08.2018

# Abstract

Computer-aided drug design is applied at an early stage of the drug development process for target validation, hit identification, hit-to-lead optimization and lead optimization. The current work illustrates these applications in the context of enzyme inhibitors development. Specifically, inhibitors targeting two families of therapeutically interesting zinc-dependent enzymes are discussed. Firstly, histone deacetylase (HDAC) inhibitors marketed for cancer treatment and potentially applicable for parasitic and other diseases. Secondly, UDP-3-*O*-(*R*-3-hydroxymyristoyl)-*N*-acetylglucosamine deacetylase (LpxC) inhibitors, which are emerging antibacterial agents. This thesis mainly focuses on computer-aided drug design contribution for the development of the above mentioned inhibitors. It narrates how novel hits for the antiparasitic target *Schistosoma mansoni* HDAC8 (SmHDAC8) were discovered using virtual screening and how their optimization was guided by molecular docking, structure-based design and binding free energy calculations. It also demonstrates application of homology modeling, molecular docking and molecular dynamics simulation to assist target validation by providing structural analysis of parasitic and human HDACs. Finally, it describes how molecular docking was used to rationalize the biological activity of anticancer HDAC6 inhibitors and antibacterial LpxC inhibitors and to guide their optimization. Thus, these results show how computer-based methods helped to accelerate and rationalize the development of inhibitors of zinc-dependent enzymes.

**Keywords:** zinc-dependent enzymes, HDAC, LpxC, inhibitors, computer-aided drug design, molecular modeling, homology modeling, molecular docking, molecular dynamics simulation, binding free energy calculations, virtual screening, antiparasitic, anticancer, antibacterial, epigenetics

# Kurzfassung

Computergestütztes Wirkstoffdesign wird in einem frühen Stadium der Medikamentenentwicklung zur Target Validierung, Hit Identifikation, Hit-to-Lead-Optimierung und Lead-Optimierung eingesetzt. Die vorliegende Arbeit veranschaulicht diese Anwendungen im Kontext der Entwicklung von Enzyminhibitoren. Es werden Inhibitoren diskutiert, die zu zwei Familien von therapeutisch interessanten Zink-Enzymen gehören. Erstens, Histon-Deacetylase (HDAC) Inhibitoren zugelassen für die Krebsbehandlung und potenziell anwendbar für parasitäre und weitere Krankheiten. Zweitens, UDP-3-O-(*R*-3-Hydroxymyristoyl)-*N*-Acetylglucosamin-Deacetylase (LpxC) Inhibitoren, die neue antibakteriell wirksame Arzneistoffkandidaten sind. Die vorliegende Arbeit konzentriert sich hauptsächlich auf den Beitrag des computergestützten Wirkstoffdesigns zur Entwicklung der oben genannten Inhibitoren. Sie berichtet, wie neuartige Hits für das antiparasitäre Target (SmHDAC8) mithilfe von virtuellem Screening entdeckt wurden und wie ihre Optimierung durch molekulares Docking, strukturbasiertes Wirkstoffdesign und freie Bindungsenergie Berechnungen gestützt wurde. Es demonstriert auch die Anwendung von Homologie-Modellierung, molekularem Docking und Moleküldynamik Simulation zur Unterstützung der Target Validierung durch Bereitstellung einer strukturellen Analyse von parasitären und humanen HDACs. Schließlich wird beschrieben, wie das molekulare Docking die biologische Aktivität von HDAC6 Inhibitoren und antibakteriellen LpxC Inhibitoren erklären kann und deren Optimierung unterstützen kann. Somit zeigen diese Ergebnisse wie computerbasierte Methoden die Entwicklung von Zink-Enzyme Inhibitoren beschleunigen und rationalisieren konnten.

**Schlagwörter:** Zink-Enzyme, HDAC, LpxC, computergestütztes Wirkstoffdesign, molekulare Modellierung, Homologie-Modellierung, molekulares Docking, freie Bindungsenergie Berechnung, virtuelles Screening, antiparasitäre, antikrebs, antibakterielle, Epigenetik

# Acknowledgments

My exciting and challenging PhD-time was guided and supported by many people, whose contribution I would like to gratefully acknowledge. First and most of all, I want to thank my "Doktorvater" Prof. Dr. Wolfgang Sippl for giving me multiple interesting tasks, for always having time to discuss scientific problems, for teaching me and helping me grow, for being tolerant, patient and kind, and for being a great example.

I am also very grateful to my colleagues. They created a professional, yet friendly atmosphere, were helpful and readily shared their experience. Especially I want to thank my friend and colleague Dr. Inna Slynko who supported me through the most difficult time at the beginning of my work. Also my special thanks to Dr. Dina Robaa for her valuable advices and critical comments.

I would like to express my sincere gratitude to our numerous collaborators, especially to those with whom we had the most intense communication Prof. Dr. Manfred Jung, Prof. Dr. Raymond J. Pierce, Dr. Christophe Romier and Prof. Dr. Ralph Holl. Many thanks also to our project coordinators for their hard work. I enjoyed participating in SEtTReND and A-ParaDDisE projects coordinated by Prof. Pierce as it did not only give me valuable experience but also a wonderful feeling of being a part of something big and meaningful. It was a great pleasure to participate in EUROPIN project coordinated by Prof. Dr. Gerhard F. Ecker as well. During the time of this project I got critical evaluation of my work, extensive training and an opportunity to communicate with professionals from academia and industry.

Last, but not least I would like to thank my family and friends for their support. I am grateful to my husband, who I can count on and who makes me happy for many years. I am especially grateful to my little son for the joy that he brings to my life. I thank my parents who raised me and gave me freedom to choose my own path in life and career. I thank the family of my husband who have always been supportive and kind. I thank my friends scattered around Europe for sharing hard and good times with me.

I think I am lucky to be surrounded by so many great people during my PhD who helped me on professional and personal level. I do not take it for granted. I appreciate it and I always will.

*"The human mind is like a parachute. It works best when it is open."*

Paul Janssen

# Contents

<b>1. Introduction.....</b>	<b>1</b>
1.1. Zinc-Dependent Enzymes.....	1
1.2. HDACs.....	3
1.3. LpxCs.....	9
1.4. Design of HDAC and LpxC Inhibitors.....	11
<b>2. Aim of the Work.....</b>	<b>17</b>
<b>3. Methods and Materials.....</b>	<b>18</b>
3.1. Computer-Aided Drug Design.....	18
3.2. Homology Modeling.....	18
3.3. Molecular Docking.....	19
3.4. Molecular Dynamics Simulation.....	20
3.5. Binding Free Energy Calculation.....	21
3.6. Virtual Screening.....	21
3.7. <i>In vitro</i> Testing.....	22
<b>4. Results and Discussion.....</b>	<b>25</b>
4.1. Discovery of Inhibitors of <i>Schistosoma Mansoni</i> HDAC8 by Combining Homology Modeling, Virtual Screening and <i>In Vitro</i> Validation.....	25
4.2. Molecular Basis for the Antiparasitic Activity of a Mercaptoacetamide Derivative that Inhibits Histone Deacetylase 8 from the Human Pathogen <i>Schistosoma mansoni</i> .....	26
4.3. Structure-Based Design and Synthesis of Novel Inhibitors Targeting HDAC8 from <i>Schistosoma mansoni</i> for the Treatment of Schistosomiasis.....	27
4.4. Isophthalic Acid-Based HDAC Inhibitors as Potent Inhibitors of HDAC8 from <i>Schistosoma mansoni</i> .....	28
4.5. Homology Modeling of Parasite Histone Deacetylases to Guide the Structure-Based Design of Selective Inhibitors.....	29
4.6. Evolutionary Relationships among Protein Lysine Deacetylases of Parasites Causing Neglected Diseases.....	30
4.7. Targeting Histone Deacetylase 8 as a Therapeutic Approach to Cancer and Neurodegenerative Diseases.....	31
4.8. Synthesis and Biological Investigation of Oxazole Hydroxamates as Highly Selective Histone Deacetylase 6 (HDAC6) Inhibitors.....	32

4.9. 2-Benzazolyl-4-piperazin-1-ylsulfonylbenzenecarbohydroxamic Acids as Novel Histone Deacetylase-6 Inhibitors with Antiproliferative Activity.....	33
4.10. Synthesis, Biological Evaluation and Molecular Docking Studies of Benzyloxyacetohydroxamic Acids as LpxC Inhibitors.....	34
4.11. Synthesis and Biological Evaluation of Enantiomerically Pure Glyceric Acid Derivatives as LpxC Inhibitors.....	35
<b>5. Conclusions.....</b>	<b>36</b>
5.1. Hit Identification for SmHDAC8.....	36
5.2. Optimization of SmHDAC8 Inhibitors.....	38
5.3. Assisting Target Validation of Parasitic HDACs.....	39
5.4. Optimization of Human HDAC6 Inhibitors.....	40
5.5. Optimization of Bacterial LpxC Inhibitors.....	40
5.6. General Conclusions.....	41
<b>6. References.....</b>	<b>42</b>
<b>7. List of Figures.....</b>	<b>49</b>
<b>8. List of Abbreviations.....</b>	<b>50</b>
<b>9. Appendix.....</b>	<b>51</b>
9.1. List of Zinc-Dependent Enzymes.....	51
9.2. Full-Text Manuscripts.....	57



# 1. Introduction

## 1.1. Zinc-Dependent Enzymes

Zinc is a micronutrient essential for the growth of all forms of life. It is fundamentally important for cellular regulation, since it acts as a messenger for information transfer within cells and between cells [1]. Furthermore, it is a cofactor required for the catalytic activity of numerous metalloenzymes, which are called zinc-dependent enzymes. More than 300 of these proteins have been discovered so far [2], but at least ten times more of them probably exist [1]. They differ greatly in structure and function, are represented in all six classes of enzymes and are found in various species of all phyla [2].

An extended list of zinc-dependent enzymes based on data from ExPASy - ENZYME database [3] is provided in Appendix 9.1 to give an overview of this large group of metalloproteins. For example, human alcohol dehydrogenase participating in alcohol metabolism belongs to class 1 enzymes oxidoreductases [4]. Human protein farnesyltransferase, performing post-translational protein prenylation regulating cell growth, movement and protein trafficking, is a representative of class 2 enzymes transferases [5]. Most of the zinc-dependent enzymes belong to class 3 enzymes hydrolases. Subclass 3.4 peptidases contains the largest number of representatives including leukotriene A4 hydrolase (an important player in the immune system) [6] and angiotensin converting enzyme (controls blood pressure) [7]. Enzymes investigated in this work human and parasitic histone deacetylase (HDAC) and bacterial UDP-3-O-(*R*-3-hydroxymyristoyl)-*N*-acetylglucosamine deacetylase (LpxC) also belong to class 3 enzymes and are classified as subclass 3.5.1 hydrolases acting on linear amides [8]. They will be discussed in details later. Zinc-dependent enzymes are less represented in classes 4-6, but some examples are known. For instance, human carbonic anhydrase involved in respiration, acid-base homeostasis and other processes is a class 4 enzyme lyase [9]. Phosphomannose isomerase is an example of class 5 enzymes isomerases catalyzing reversible isomerization of mannose-6-phosphate and fructose-6-phosphate [10]. A representative of class 6 enzymes ligases is pyruvate carboxylase, which transfers an activated carboxyl group between distinct active sites [11]. These examples illustrate the diversity of zinc-dependent enzymes and their distribution among enzyme classes.

Although all zinc-dependent enzymes contain zinc, its function and surrounding may vary. Thus the binding sites of the zinc ion are classified into three groups: catalytic, co-catalytic and structural. Catalytic zinc-binding sites contain one zinc ion, which is directly involved in the catalytic mechanism. This zinc ion generally coordinates four ligands, three of which are nitrogen, oxygen or sulfur ligands from protein amino acid residues and the fourth ligand is a water molecule. This water molecule either participates catalytically in the reaction or is replaced by a substrate. Co-catalytic zinc-binding sites contain two or more metal ions at least one of which is zinc. The metal ions are usually in close proximity and bridged by a common ligand, which is often a water molecule or a carboxylate ligand. Finally, structural zinc-binding sites contain one zinc ion, which performs a structural role (stabilizes protein conformation). Structural zinc ions are typically coordinated by four ligands from protein residues, preferably cysteines [2, 8]. Catalytic, co-catalytic and structural zinc-binding sites can be targeted to inhibit the activity of zinc-dependent enzymes.

Inhibitors of many zinc-dependent enzymes are either used as drugs or investigated as drug candidates. For instance, angiotensin-converting enzyme inhibitors are used to treat hypertension and heart failure [7], histone deacetylase inhibitors are approved for cancer treatment [12], carbonic anhydrase inhibitors are clinically used as antiglaucoma agents, diuretics, antiepileptics, in the management of mountain sickness, ulcers, neurological disorders, osteoporosis [9]. The search for new inhibitors and their optimization is mainly focused on targeting the catalytic zinc ions with molecules containing a zinc-binding group (ZBG). This group is a warhead which coordinates the active site metal ion and is crucial for inhibitory activity. By analysis of the X-ray structures deposited in the Protein Data Bank, K. Kawai and N. Nagata collected a number of zinc binding groups, which are binding to the zinc ion in zinc-dependent enzymes [13]. Besides the well-known ZBGs, such as hydroxamate, sulfonamide, carboxylate, carbamate, phosphate, thiol, diol and imidazole, also more exotic groups were identified, such as *N*-substituted hydroxamate, triazole, pyrazole, pyridine, uridine, barbiturate, hydantoin, sulfoxide, urea, boronic acid, mercaptoacyl, nitro, 8-hydroxyquinoline, 1-hydroxy-2-sulfanylpuridinium. As shown in the same study, all the ZBGs interact with the zinc ion through oxygen, nitrogen or sulfur atom. Since some ZBGs contain more than one heteroatom which interacts with zinc, they can bind either in a monodentate or a bidentate manner. Usually there is a clear preference for a certain binding mode. This is the case with sulfonamides, which prefer monodentate interactions and hydroxamates, who mostly bind as bidentate ligands. In contrast, carboxylates show both mono- and bidentate interactions.

On one hand, the presence of the ZBG in the structure of inhibitors enables them to bind tightly in the binding pocket of the target. On the other hand, there are concerns that the ZBGs are not specific to the desired target, but are also able to inhibit off-target metalloenzymes and even capture the metal ions from metal transport proteins. To look into the selectivity of metalloenzyme inhibitors, J. A. Day and S. M. Cohen tested several known inhibitors bearing different metal-binding groups on a panel of targets [14]. The targets included several zinc-dependent enzymes (carbonic anhydrase, angiotensin converting enzyme, histone deacetylase, matrix metalloproteinases and botulinum neurotoxin), an iron-dependent enzyme (5-lipoxygenase), a copper-dependent enzyme (mushroom tyrosinase), a magnesium-dependent enzyme (human deficiency virus integrase) and an iron transport protein (transferrin). Their results show, that the off-target inhibition is limited even in case of identical metal-binding group. Also marketed drugs displayed higher selectivity than early stage lead compounds. This suggests that inhibitor selectivity is coming from the combination of a metal-binding group and the backbone of inhibitor. Furthermore, it appears that the non-specific activity of metalloenzyme inhibitors is comparable to off-target effects of inhibitors of other enzymes. To conclude, the ZBG is a key feature of inhibitors of zinc-dependent enzymes, which limits their chemical space. For a specific interaction of the inhibitor with the target, a suitable ZBG fitting to the binding pocket environment has to be chosen and enhanced by a selectivity-bearing backbone. In this work we focus on design of inhibitors for two families of zinc-dependent enzymes: HDACs and LpxCs.

## 1.2. HDACs

The superfamily of histone deacetylases (HDACs) is large and ancient. It originates in prokaryotes and is represented in various eukaryotic organisms, including mammals. The human genome encodes eleven HDAC isoforms with highly conserved deacetylase domain (also called catalytic domain) containing the catalytic zinc-binding site. These proteins are also known as classical HDACs or zinc-dependent HDACs. They are subdivided into four classes: class I, class IIa, class IIb and class IV. Besides them, 7 homologues of another group of deacetylases, the sirtuins, share the same name. Sirtuins are called class III HDACs or NAD<sup>+</sup>-dependent HDACs, however, they have a distinct structure and catalytic reaction mechanism [15, 16]. Since sirtuins are beyond the focus of the current work, they will not be discussed here and the name HDACs will be used for classical HDACs only.

HDACs of each class have different subcellular localization and expression patterns. Class I HDACs (HDAC1, HDAC2, HDAC3 and HDAC8) and a single class IV member HDAC11 are localized predominantly in the nucleus, class IIa (HDAC4, HDAC5, HDAC7 and HDAC9) - both in the nucleus and cytoplasm, while class IIb (HDAC6 and HDAC10) - in the cytoplasm [15, 17]. Class I HDACs are expressed ubiquitously. In contrast, class IIa HDACs have restricted expression patterns: HDAC4 is highly expressed in the brain and growth plates of the skeleton, HDAC5 and HDAC9 are highly enriched in the muscles, heart and brain, HDAC7 – in the endothelium and T-cell precursors [15]. HDAC6, belonging to class IIb, is ubiquitously expressed [16], while HDAC10, the second member of the same class, is highly expressed in the liver, spleen and kidney [18]. HDAC11, a class IV HDAC, is enriched in the kidney, heart, brain, muscle, and testis [17].

The spectrum of the biological functions of HDACs is broad and is not limited to histone deacetylation. When the first human class I HDACs were discovered, it was found that they participate in epigenetic regulation of gene transcription by deacetylation of histones. Nowadays it is known that the substrates of HDACs are not only histones, but also non-histone proteins such as tumor suppressor protein p53, transcription factors,  $\alpha$ -tubulin, chaperone protein Hsp90, cortical actin binding protein, one of the core proteins of the cohesin complex SMC3 [16] and even polyamines [18]. Furthermore, HDACs have been suggested to be responsible not only for deacetylation, but also for removal of formyl, propionyl, butyryl, crotonyl, valeryl, octanoyl, dodecanoyl and myristoyl groups. Therefore, HDACs are sometimes referred to more generally, for example, as protein-lysine deacetylases or as histone deacylases [16, 18-20]. In addition to that, it was shown that highly purified class IIa HDACs demonstrate very weak enzymatic activity. It was hypothesized that their major role is non-catalytic, possibly as epigenetic readers [15, 21]. To conclude, in contrast to what the name suggests, histone deacetylases cannot be simply defined as enzymes which deacetylate histones. Members of the family have multiple biological functions, which in some cases do not include deacetylation of histones. Despite that, their traditional name "histone deacetylases" (HDACs) is the most recognized one.

The functionally diverse family of HDACs is united by its structural similarity. According to the amino acid sequence analysis, all HDAC isoforms contain a conserved deacetylase domain. Class I and class IV HDACs consist almost entirely of a deacetylase domain with short N- and C-terminal extensions and are approximately 400 amino acids long. Class IIa HDACs have large N-terminal extensions in addition to the C-terminal deacetylase domain and are around 1000 amino acids long. Class IIb HDACs are around 1200 (HDAC6) and 700 (HDAC10) amino acids long [15].

They differ from other human HDACs by having two deacetylase domains. In addition, HDAC6 also harbors a unique zinc finger domain [15, 18, 22]. It is not clear if both deacetylase domains of HDAC6 are catalytically active. It has been suggested that only the second domain has enzymatic activity, although both domains might be required for the functioning of the enzyme [22]. In case of HDAC10, the first domain functions as polyamine deacetylase, whereas the second is a pseudo-deacetylase domain, which lacks conserved features and enzymatic activity [18]. Thus, at least one deacetylase domain is present in every HDAC and is a key structural feature of this protein family.

Crystal structures solved for class I, class IIa and class IIb HDACs showed that the deacetylase domain has a highly conserved architecture [18, 22, 23]. As an example, one of the first published crystal structures of HDAC8 is represented in Figure 1. It shows that HDAC8 has a single domain with  $\alpha/\beta$  fold consisting of a central eight-stranded parallel  $\beta$ -sheet sandwiched between several  $\alpha$ -helices [24]. These secondary structure elements, which are partially conserved across the HDAC family, are connected by loops. Some of the loops are highly similar, whereas most of them have diverse lengths and conformations. A funnel-shaped cavity located at the center of the domain is present in every HDAC crystal structure and is called the lysine-binding channel. A set of flexible loops form protein interaction interfaces at the rim of the channel. The channel itself is around 11 Å deep and can be extended by various sub-pockets depending on the HDAC isoform, such as the foot pocket in class I HDACs. A combination of conserved residues organized around the zinc ion are situated at the bottom of the channel. They participate in the catalytic process of the enzymatically active HDACs [23, 25].

The catalytic mechanism of HDACs is illustrated in Figure 2, showing as an example the deacetylation of substrate acetyllysine by HDAC6 as deduced from recently published crystal structures. The catalytic zinc ion of the resting enzyme is tetra-coordinated by three protein amino acid residues (D649, H651 and D742) and a water molecule (Fig. 2a). The reaction starts when the carbonyl of the acetyllysine approaches the zinc ion near the zinc-bound water molecule (Fig. 2b). This water molecule, which is activated by H610 and the zinc ion, performs a nucleophilic attack on the acetyllysine carbonyl group yielding a tetrahedral intermediate (Fig. 2c). The intermediate collapses when the general acid, namely the protonated H611, protonates the leaving amino group (Fig. 2d) [22]. A similar reaction mechanism is expected for class I HDACs [25]. The loss of activity of class IIa HDACs is explained by the replacement of the transition-state stabilizing tyrosine by a histidine residue [23].

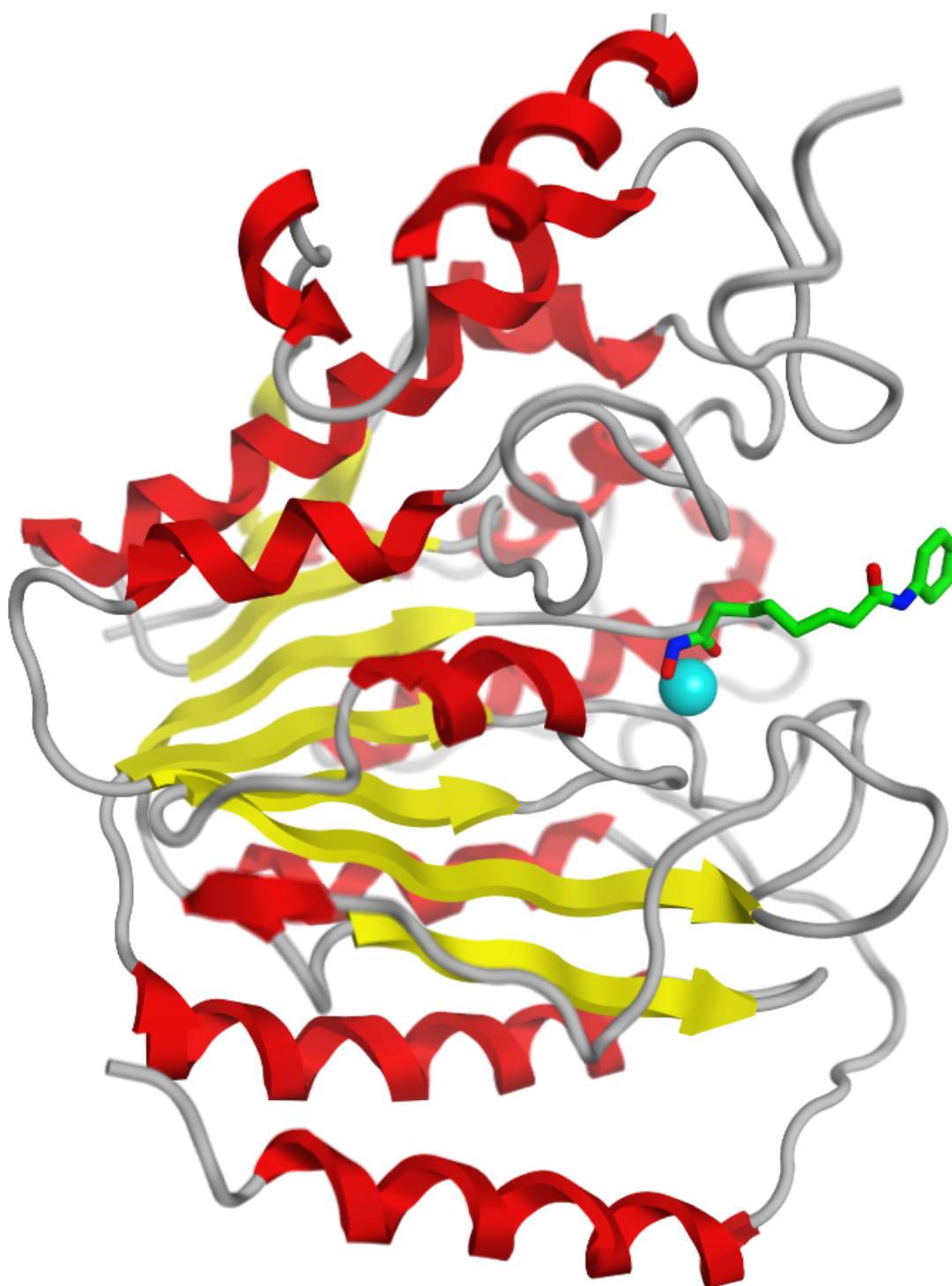


**Figure 1.** Crystal structure of human HDAC8 with the inhibitor vorinostat (PDB ID 1T69) representing the common architecture of HDAC deacetylase domain. The central  $\beta$ -sheet (yellow arrows) is sandwiched by  $\alpha$ -helices (red helices) and surrounded by loops (gray ribbons). The catalytic pocket is occupied by vorinostat (stick representation, green carbon atoms), which is interacting with the catalytic zinc ion (cyan sphere).

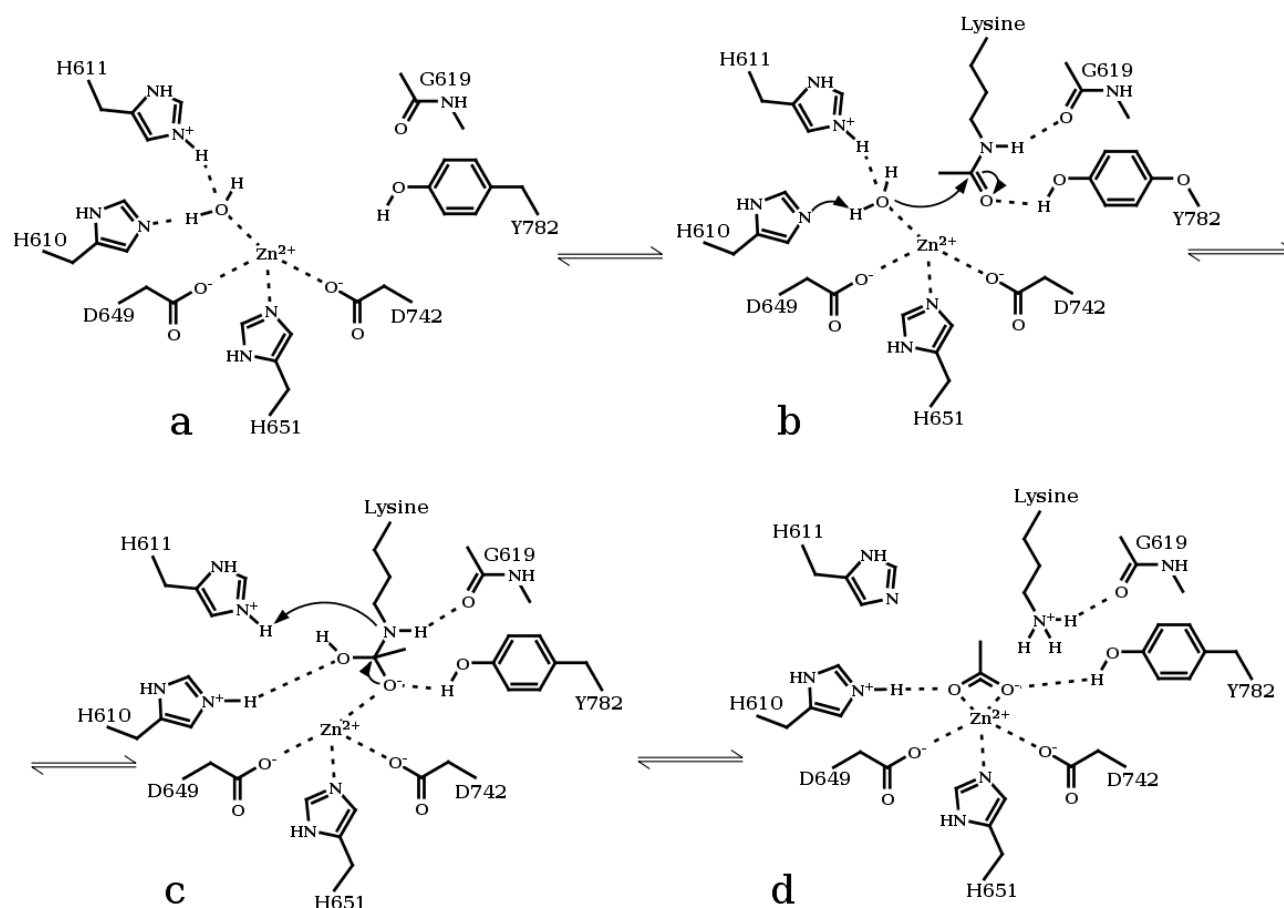


**Figure 2.** Putative catalytic mechanism steps (a-d) of the deacetylation reaction in HDAC6.

The catalytic activity of HDACs is their key function, which is important to perform physiological roles of HDACs. These are demonstrated by knockout studies on mice [15]. Deletion of each member of the class I HDACs leads to embryonic or perinatal lethality. Genetic depletion of class IIa HDACs also results in dramatic phenotypes. Namely, HDAC4-null mice die during the first week due to defects in bone formation. HDAC5 and HDAC9 knockouts are viable, but have cardiac defects. The lack of HDAC7 results in embryonic lethality due to vascular disruption. Surprisingly, deletion of HDAC6 does not cause an obvious phenotype. However, the levels of acetylated tubulin are increased in those animals, which indicates the importance of HDAC6 in protein folding and cytoskeletal dynamics. HDAC10- and HDAC11-knockout mice are viable [16].

The dramatic phenotypes of most HDAC genes deletion suggest that HDACs might not be promising drug targets, however this is not true. Inhibition of HDACs *in vivo* is unexpectedly well tolerated. A possible explanation for this phenomenon would be that inhibitors block the enzymatic activity of HDACs, but do not necessarily prevent them from participation in the multiprotein transcriptional complexes. Indeed, several HDAC inhibitors have been approved for the treatment

of cancer in recent years and many drug candidates are in clinical trials [26]. Moreover, HDAC inhibitors provide benefit in multiple disease states including cancer, neurodegenerative and immunological diseases, traumatic shock, cardiac hypertrophy, viral and parasitic infections [15, 27]. Thus, HDACs are exciting drug targets with multiple applications.

Usually, the human HDACs discussed here are the targets for drug development. However, in the case of parasitic infections, the actual targets are the pathogen's HDACs, while human HDACs are rather off-targets potentially causing unwanted side effects. So far HDAC homologues have been identified in several major human-infecting parasites, including *Plasmodium falciparum*, *Trypanosoma brucei*, *Schistosoma mansoni* and *Leishmania major* [27]. Functionally characterized HDACs play important roles in parasites growth and development and some of them are crucial for the survival of the pathogens. Due to the therapeutic relevance of parasitic HDACs, their representative will be introduced in this chapter as an example.

One of the parasitic HDACs investigated in more details is *Schistosoma mansoni* HDAC8 (SmHDAC8). This enzyme is expressed at all life-cycle stages of the parasite [28] and its down-regulation leads to the decreased capacity of the pathogen to survive and mature in infected mice [29]. The essential role of SmHDAC8 in parasite infectivity suggests that it could be targeted by HDAC inhibitors for antiparasitic treatment. Several non-selective HDAC inhibitors have been shown to induce mortality of *S. mansoni* in culture medium [29, 30], which proves that they are able to penetrate this parasite and probably inhibit its HDACs. However, it should be taken into account that human HDACs might also be affected *in vivo*. Further advantage of SmHDAC8 as a drug target lies in its structural features which provide an opportunity to design parasite-specific inhibitors. Firstly, the SmHDAC8 F151 side chain adopts two conformations: the flipped-in conformation conserved in all available human HDAC structures and the parasite-specific flipped-out conformation. Secondly, the side chain of the catalytically important amino acid residue Y341 in SmHDAC8 is observed in an unusual conformation where it points towards the rim of the binding pocket. Thirdly, SmHDAC8 contains H292 in the binding pocket in contrast to human HDAC8, which has M274 at the corresponding position. Specific residue H292 and the unusual Phe151 and Y341 side chain plasticity ensure the unique architecture of the SmHDAC8 binding pocket and can be exploited by structure-based inhibitor design [29]. All this evidence provides the proof of concept that targeting SmHDAC8 can be used to treat parasitic infections and adds it to the list of druggable HDACs.



### 1.3. LpxCs

UDP-3-*O*-(*R*-3-hydroxymyristoyl)-*N*-acetylglucosamine deacetylases (LpxCs) are zinc-dependent enzymes highly conserved and exclusively found in Gram-negative bacteria. They do not only lack sequence homology with any mammalian proteins but are also structurally unique [31]. The first published crystal structure of LpxC from *Aquifex aeolicus* revealed that this protein has a novel fold which is not related to other zinc hydrolases [8]. The subsequently solved structures of LpxCs from other microorganisms (*Escherichia coli*, *Pseudomonas aeruginosa* and *Yersinia enterocolitica*) shared the same architecture [32], which is demonstrated in Figure 3 by the X-ray structure of *E. coli* LpxC. The protein consists of two domains of identical topology. Each domain contains a layer of five-stranded  $\beta$ -sheet and a layer of  $\alpha$ -helices. These two domains form a  $\beta$ - $\alpha$ - $\beta$  fold with the helices sandwiched between the two  $\beta$ -sheets. Also each domain contains a unique structural element which is named insert (insert I of domain I and insert II of domain II respectively). The substrate binding site is located at the interface of the two domains. It contains the zinc ion which is required for the catalytic activity of LpxC [33].

The enzymatic function of LpxCs is utilized in the biosynthesis of lipid A, which is a glucosamine-based phospholipid comprising the outer membrane of Gram-negative bacteria. Lipid A protects microorganisms from antibiotics and detergents and is essential for their survival. With few exceptions, bacteria which lack lipid A are not viable. Mutants with reduced lipid A biosynthesis grow slowly and are sensitive to antibiotics. Besides, lipid A is a powerful endotoxin causing a life-threatening condition, namely septic shock. Therefore, inhibition of lipid A biosynthesis represents a promising approach to handle Gram-negative bacterial infections and sensitizing pathogens to other antibiotics. Additionally, the complications of septic shock may be reduced during treatment due to the inhibition of the endotoxin production [31].

Lipid A biosynthesis is a ten-step process, which occurs in the cytosol on the inner surface of the inner membrane [31]. LpxCs catalyze the second step of this pathway, namely, the hydrolysis of UDP-3-*O*-myristoyl-*N*-acetylglucosamine to UDP-3-*O*-(*R*-hydroxymyristoyl)-glucosamine and acetate [8]. LpxC is particularly attractive among enzymes of the lipid A biosynthesis pathway due to its regulatory role. Both increasing and decreasing of LpxC activity leads to lethality of *E. coli* [31]. Treatment with LpxC inhibitors cures mice infected with a lethal intraperitoneal dose of *E. coli* [34]. Moreover, LpxC inhibitors are curative in murine model of bubonic plague, one of the most severe human infections caused by the Gram-negative bacteria *Yersinia pestis* [35].

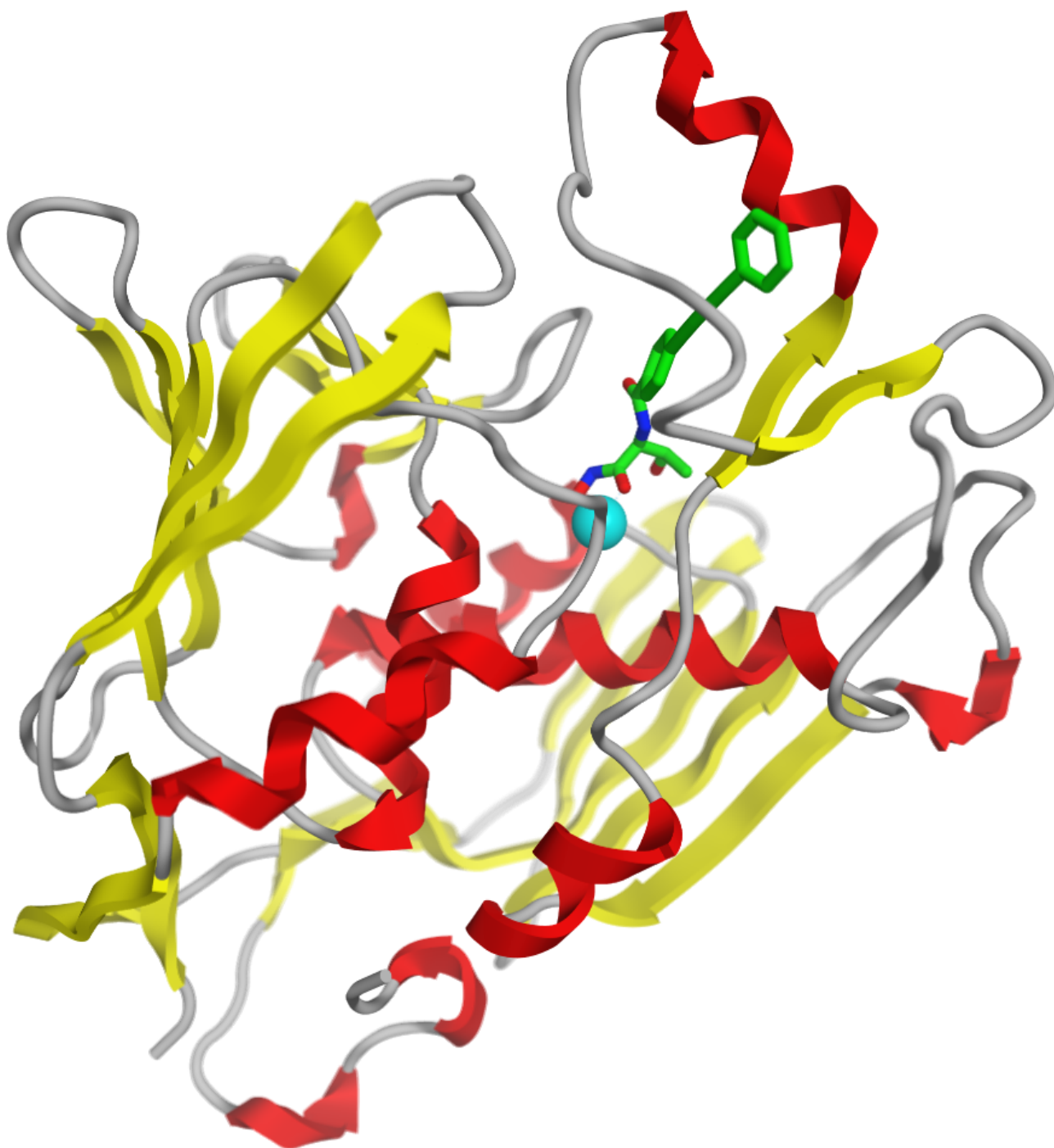


**Figure 3.** Crystal structure of *E. coli* LpxC with the inhibitor LPC-009 (PDB ID 3P3G) representing the common architecture of LpxC fold. The catalytic pocket contains the catalytic zinc ion (cyan sphere) and is occupied by LPC-009 (stick representation, green carbon atoms). It is located at the interface of two homologous domains. These domains consist of  $\beta$ -sheet (yellow arrows) and  $\alpha$ -helices (red helices) connected by loops (gray ribbons) and together form a unique  $\beta$ - $\alpha$ - $\alpha$ - $\beta$  sandwich fold.

The catalytic deacetylation reaction mechanism of LpxC is shown in Figure 4. First, the zinc-bound water molecule is activated by E78 for nucleophilic attack on the carbonyl group of the acetylated substrate (Fig. 4a). This results in the formation of a tetrahedral intermediate, which is stabilized by T191 through a hydrogen bond. Further H265 donates a proton to the amine of the leaving group (Fig. 4b) [31].

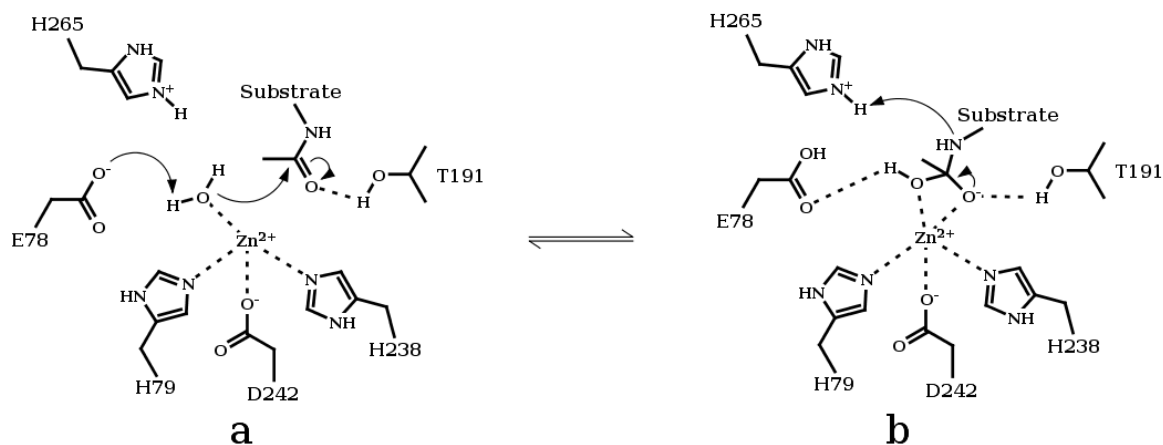


**Figure 4.** Putative catalytic mechanism steps (a-b) of the deacetylation reaction by *E. coli* LpxC.

The unique structure and biological importance of LpxCs makes them intriguing drug targets. Due to the bacteria-specific architecture of LpxCs, it should be possible to design highly selective inhibitors with limited off-target effects and human toxicity [31]. Furthermore, LpxCs are essential for the survival of Gram-negative bacteria as shown by *in vitro* and *in vivo* experiments [31, 35]. Thus, LpxCs are validated targets for the development of antibacterial agents.

## 1.4. Design of HDAC and LpxC Inhibitors

As mentioned before, inhibitors of zinc-dependent enzymes usually consist of a ZBG and the backbone of the molecule, attached to it. HDACs and LpxC inhibitors are no exceptions of this rule. Several example structures of HDAC and LpxC inhibitors are shown in Figure 5. All of them contain a ZBG, which is their essential feature. This group is the warhead of the inhibitors. It coordinates the catalytic zinc ion of the target enzyme and prevents substrate binding [25, 36]. The nature of the ZBG heavily influences the inhibitor activity, selectivity and toxicity. Therefore, choosing a suitable ZBG is the first and most important step in *de novo* design of HDAC and LpxC inhibitors.

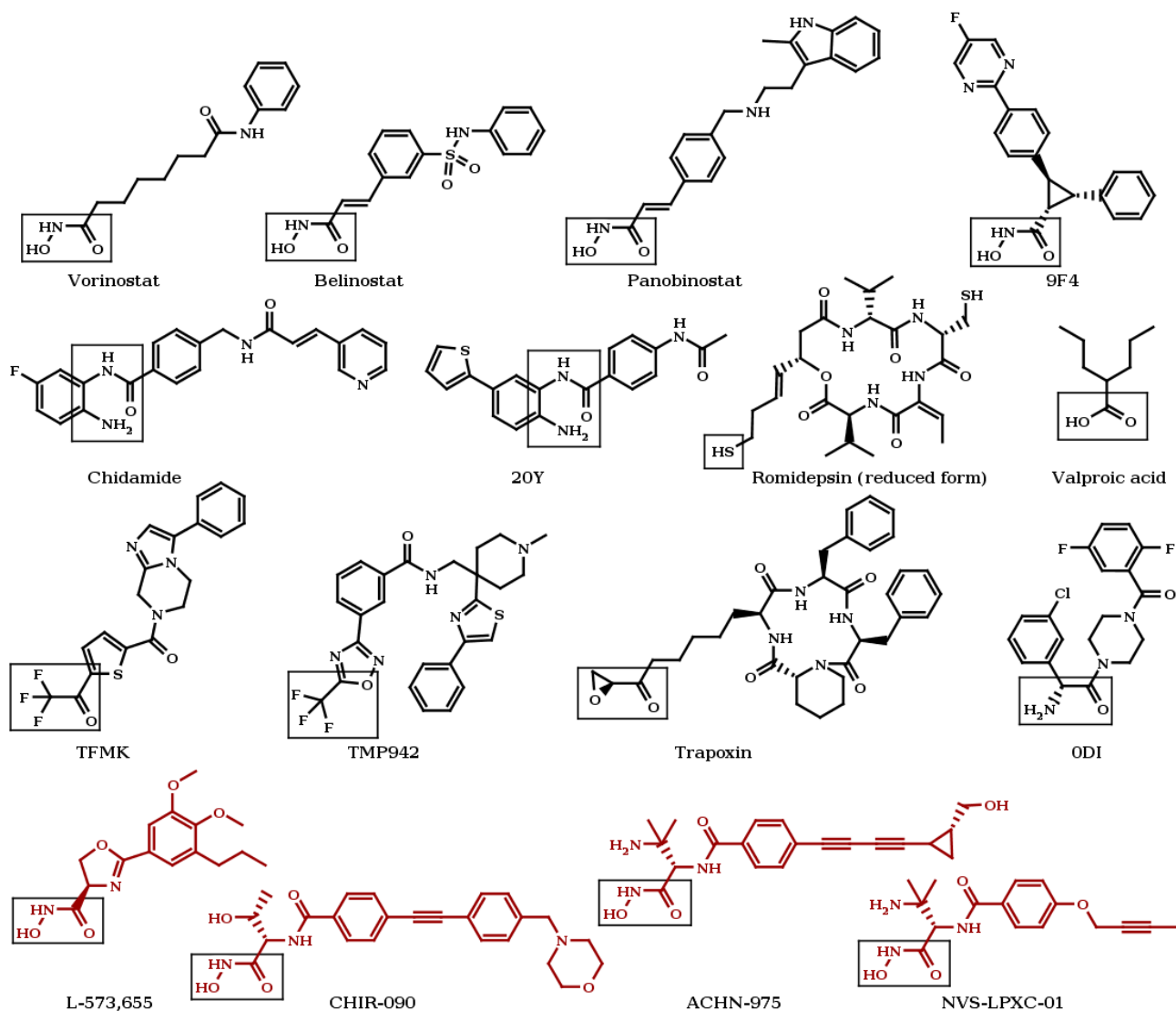


**Figure 5.** Representative structures of HDAC and LpxC inhibitors. Inhibitors are sorted by target (HDAC inhibitors – black, LpxC inhibitors – red) and ZBG (framed).

The most common ZBG of both HDAC and LpxC inhibitors is hydroxamic acid [25, 36]. It is also present in approved drugs (vorinostat, belinostat, panobinostat) (Figure 5). Hydroxamic acids are usually preferred over other ZBGs due to their positive properties, such as remarkable zinc binding capability and good *in vivo* activity. However, hydroxamic acids are not perfect and are often criticized due to their poor pharmacokinetic properties (rapid clearance) and side effects including mutagenicity [37]. Negative properties of hydroxamic acid containing drugs can be tolerated when they are used to treat life-threatening or acute conditions like cancer or acute infections [31, 37]. As for the treatment of non-severe chronic diseases, it might be reasonable to also consider alternative ZBGs (and their positive and negative aspects). For instance, HDAC inhibiting approved drugs contain such ZBGs as *ortho*-aminoanilide (chidamide), thiol (romidepsin) and carboxylic acid (valproic acid) (Figure 5) [37]. The ZBGs of inhibitors co-crystallized with

HDACs also include trifluoromethylketone (TFG) [38], trifluoromethyloxadiazole (TMP942) [39],  $\alpha,\beta$ -epoxyketone (trapoxin) [40], and amino acid derivative (ODI) [41] (Figure 5). A number of other ZBGs were discovered, but they usually bind more weakly. To sum up, various ZBGs are known to bind to the zinc ion of HDACs and LpxCs. Among them hydroxamic acid is the most wanted ZBG due to its solid advantages.

The backbone of the inhibitor adjacent to the ZBG determines the shape of the molecule and as a consequence its binding mode and selectivity. Many of the firstly discovered HDAC inhibitors had linear shape mimicking the substrate and also exhibited a similar binding mode as the substrate. Hence, they typically did not distinguish between the pockets of most HDAC isoforms and were non-selective [42, 43]. Linear (or I-shaped) HDAC inhibitors include approved drugs, e.g., vorinostat, belinostat, panobinostat, which are broad spectrum or pan-HDAC inhibitors targeting most of the HDAC isoforms in the nanomolar range [42]. As an example, the structure of the pan-HDAC inhibitor vorinostat co-crystallized with one of its targets HDAC2 is shown in Figure 6a. It can be seen, that the backbone of vorinostat occupies the hydrophobic substrate binding channel present in every HDAC, which explains the lack of selectivity [44].

Nowadays selectivity becomes more and more desirable feature of HDAC inhibitors, since there are concerns, that inhibition of multiple members of the HDAC family may cause unwanted effects. It might be possible to reduce the toxicity by targeting only one or several isoforms, which are involved in a specific pathological process [42]. Most of the early attempts to generate selective HDAC inhibitors were concentrated on the modification of the backbone of I-shaped inhibitors. This was achieved by changing either the capping group, interacting with the surface of the protein, or the linker, occupying the substrate binding channel and connecting the ZBG with the capping group [41]. These strategies are still relevant and are exploited by many research groups. Interestingly, it has been also suggested that it might be possible to achieve HDAC selective inhibition by disruption of the protein-protein interactions of HDACs relying on the capping group of inhibitors rather than on zinc coordination [45]. However, no examples of potent and selective inhibitors with this mode of action are known so far.

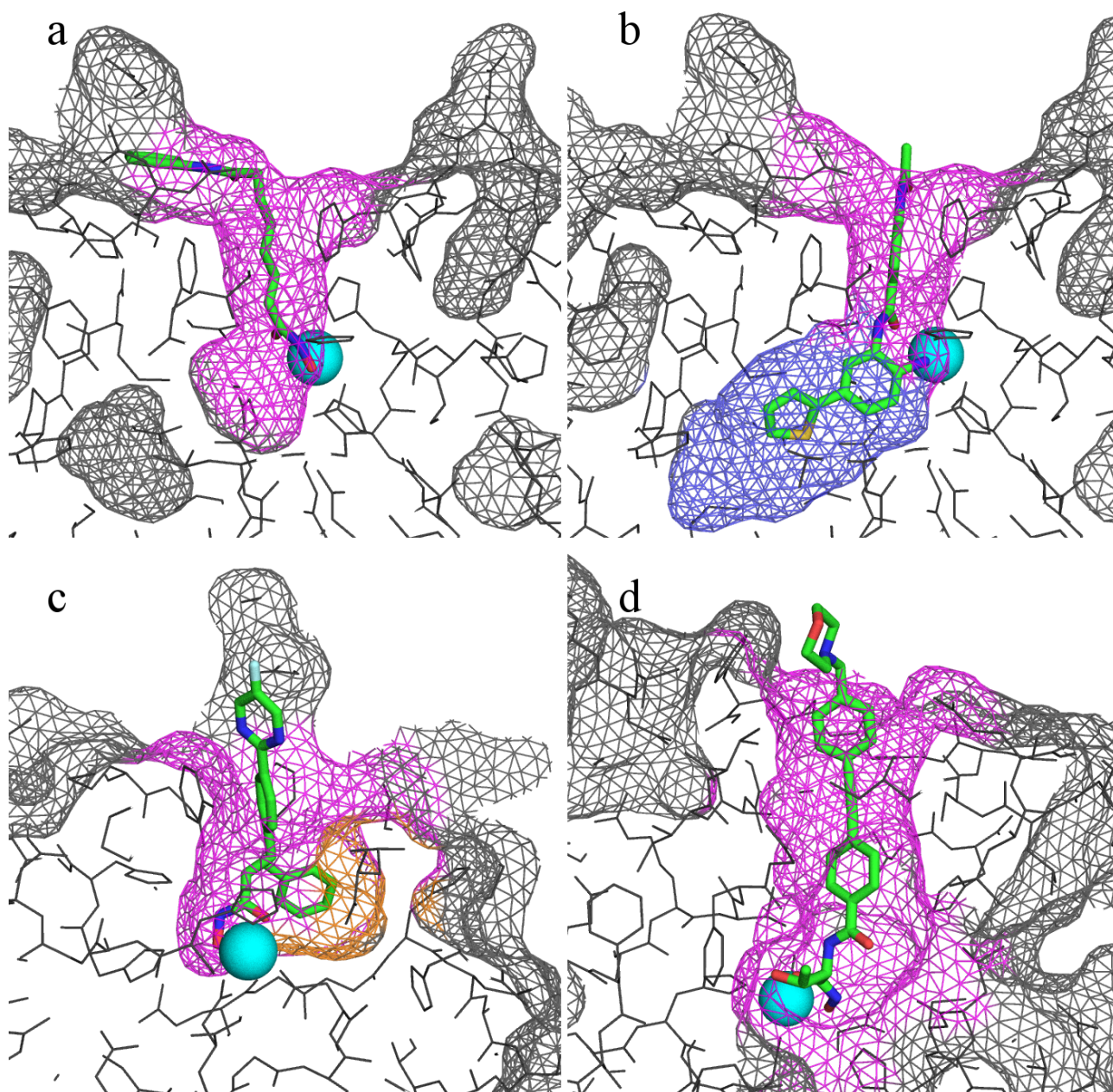


**Figure 6.** Shapes and binding modes of HDAC (a-c) and LpxC (d) inhibitors: a) I-shaped broad spectrum HDAC inhibitor vorinostat occupying the substrate binding channel in HDAC2 (PDB ID 4LXZ), b) J-shaped HDAC1-2 selective HDAC inhibitor 20Y targeting the foot pocket in HDAC2 (PDB ID 4LY1), c) L-shaped class IIa selective HDAC inhibitor 9F4 addressing the lower pocket in HDAC4 (PDB ID 4CBT), d) LpxC inhibitor CHIR-090 in *Y. enterocolitica* LpxC (PDB ID 3NZK) placed in the substrate binding channel. The surface of the protein is shown as gray wireframe, the substrate binding channel is colored magenta, the foot pocket - blue, the lower pocket - orange, protein amino acid residues are shown as gray lines, inhibitors are represented as sticks with green carbon atoms, zinc ion - as cyan sphere.



In recent years, yet another approach emerged for the design of selective HDAC inhibitors which involved changing the overall molecular shape to reach unexplored binding pocket areas. It appears that not only I-shaped inhibitors are able to bind to HDACs. Also non-linear inhibitors have been discovered, which induce protein rearrangement and opening of subtype- or class-specific subpockets. Ligand-protein interactions within these subpockets result in an increased inhibitor selectivity [25]. For example, this was observed for the HDAC1-2 selective nanomolar J-shaped inhibitor 20Y (Fig. 5) with an *ortho*-aminoanilide ZBG. As shown in Figure 6b, its thiophene "tail" is inserted in the foot pocket - a subpocket observed only in class I HDACs crystal structures. This binding mode results in high selectivity and as an additional benefit long residence time, several orders of magnitude longer than vorinostat [44]. Another example is the L-shaped hydroxamic acid ZBG containing cyclopropane derivative 9F4 (Fig. 5). It is a class IIa HDAC selective inhibitor designed to target a class-specific subpocket - the lower pocket. As seen in the crystal structure of 9F4 with HDAC4, the phenyl moiety attached to the cyclopropane ring is occupying the lower pocket (Figure 6c). This subpocket is formed by the flipped-up conformation of the side chain of histidine (H976 in HDAC4) present in all class IIa HDACs. Other HDAC isoforms contain tyrosine in the corresponding position, which is usually flipped-down keeping the lower pocket closed [46]. The discussed success stories indicate that targeting subpockets with non-linear small molecules is a promising way to design selective HDAC inhibitors.

In contrast to HDAC inhibitors, the selectivity is better achievable for LpxC inhibitors, since LpxC is a bacteria-specific enzyme not found in human. Therefore, the main focus in inhibitor design is to increase their activity. Many compounds of diverse chemotypes have been explored and reported in the literature [36] and several medicinal chemistry campaigns resulted in potent inhibitors such as L-573,655, CHIR-090, ACHN-975 and NVS-LPXC-01 (Figure 5) [47]. These inhibitors are mainly mimicking the substrate and share common structural features including the ZBG and the lipophilic moiety which addresses the hydrophobic substrate fatty acid binding channel [36]. The typical binding mode of LpxC inhibitors is demonstrated by the example of CHIR-090 co-crystallized with *Y. enterocolitica* LpxC in Figure 6d. The hydroxamic acid warhead chelates the catalytic zinc ion whereas the diphenylacetylene group is placed in the hydrophobic fatty acid binding tunnel [48].

Despite extensive drug design efforts over the past decade, only few LpxC inhibitors reached the clinic and none of them reached the market [47]. The active search for HDAC inhibitors with better properties and for new indications outside oncology also continues [45]. This underscores how challenging it is to meet the requirements for small molecule inhibitors as drugs: their

physicochemical properties should be balanced with potent activity and low toxicity [47]. Searching for these desired molecules in an endless chemical space of potential HDAC and LpxC inhibitors is like searching for a needle in a haystack. Therefore, to rationalize and accelerate research, more and more often molecular modeling approaches are exploited. For example, structure-based methods like molecular docking studies, homology modeling and molecular dynamics (MD) simulation support inhibitor design by providing putative ligand binding modes and protein structures [41, 46, 47, 49, 50]. Ligand-based methods such as quantitative structure-activity relationship (QSAR) and pharmacophore modeling have been helpful to highlight determinants of inhibitor activity and selectivity [43, 50, 51]. Molecular modeling techniques have been also incorporated into virtual screening protocols to identify new hits [52-54]. The current work adds to the list of campaigns which use computer-based methods to develop novel inhibitors of zinc-dependent enzymes HDACs and LpxCs.



## 2. Aim of the Work

The main aim of this work is to design novel inhibitors of zinc-dependent enzymes HDACs and LpxCs by applying computer-based methods. Ideally, these inhibitors should not only have a novel structure, but also be effective *in vitro* and *in vivo*, be highly selective and have little off-target or toxic effects. They should serve as drug candidates for the treatment of parasitic diseases, cancer and bacterial infections. To reach this goal different computational techniques and strategies are applied.

Firstly, a structure-based virtual screening approach is used to find novel hits for the antiparasitic target SmHDAC8. The hits then enter the drug development cycle to improve their potency, selectivity, cell permeability and further properties. Rational drug design aided by computational methods such as molecular docking and binding free energy calculation is used to guide the synthesis of new optimized inhibitors.

Secondly, homology models of relevant parasitic HDACs are built and compared to human orthologues. This is done in order to suggest promising targets for further validation and to see if SmHDAC8 inhibitors might be active on similar enzymes. Docking of known antiparasitic HDAC inhibitors to the homology models produce putative binding modes of these compounds. MD simulations test the stability of the generated homology models and protein-ligand complexes.

Thirdly, the anticancer target human HDAC6 and the antibacterial target LpxC are studied. Molecular docking is implemented to support rational design of novel HDAC6 and LpxC inhibitors and to qualitatively explain their structure-activity relationship. In addition, binding free energy calculations helpful for quantitative rationalization of obtained experimental data are carried out.

The theoretical work is supported by established collaborations with research groups performing *in vitro* and *in vivo* biological assays as well as X-ray crystallography and chemical synthesis. Collaborative research allows the development of experimentally validated protocols for computer-based design of HDAC and LpxC inhibitors, which can be repurposed for other targets. Therefore, the indirect, but equally important aim is to make contribution to the molecular modeling field.

## 3. Methods and Materials

### 3.1. Computer-Aided Drug Design

Drug design is as much science as it is art driven by creativity and intuition of the researcher [55]. Its purpose is to generate ideas or theoretical models based on available experimental data, which would guide research towards the discovery of bioactive molecules with desired properties. Nowadays the toolbox of computational chemistry, molecular modeling and chemoinformatics methods provides multiple computational instruments to assist drug design. The main challenge of computer-aided drug design is to use these instruments wisely in order to come up with a useful output corresponding to the current needs in a reasonable time.

In this work, structure-based computer-aided drug design was mainly applied, since structural information on the targets or similar proteins was available. Homology modeling, molecular docking, MD simulations, binding free energy calculations and virtual screening were chosen as the main computational methods to achieve the assigned goals. These methods are further discussed in more details.

An important part of computer-aided drug design is the visualization of molecular structures. Clear representation facilitates data perception and helps to recognize significant structural features. Pictures visualizing molecular modeling results and protein structures for current work were prepared in MOE [56] and Pymol [57]. The supplementary video, which accompanies Manuscript 4.5 and shows SmHDAC8 binding pocket flexibility, was generated in Chimera [58].

### 3.2. Homology Modeling

Amino acid sequences of target HDACs were retrieved from online databases UniProt [59], GenBank [60], SchistoDB [61] and GeneDB [62]. Sequences were further used as search queries to retrieve potential homology modeling templates from Research Collaboratory for Structural Bioinformatics Protein Data Bank (RCSB PDB, [www.rcsb.org](http://www.rcsb.org)) [63] using BLAST algorithm [64]. The final template for each target protein was chosen based on sequence similarity, X-ray resolution and protein conformation.

Initial alignment of template and target sequences was performed with CLUSTAL Omega tool [65] implemented in the UniProt database. Non-relevant fragments were removed from target sequences leaving only the parts encoding the catalytic domains. Also in some cases, large insertions (located away from the binding pocket) were cut from the target sequences, because no template was available to model them. Afterwards, alignment and template were manually refined if needed to address conserved structural features. For example, when class IIa HDACs were used as templates to model class IIb HDACs, the catalytic histidine was mutated to tyrosine in order to obtain conserved tyrosine conformation in homology model.

Homology models were built in MODELLER program [66] using the template protein structure and sequence alignment. For each target protein, five homology models were generated. They were evaluated using Discrete Optimized Protein Energy (DOPE) assessment score [67] implemented in MODELLER. The best model was chosen based on visual inspection and the DOPE score. Ramachandran plots were additionally inspected in MOE to identify areas of homology models that might require further refinement. The zinc ion was added to the models from the template structures after superimposing them. Residues were renumbered using Chimera package. Multiple sequence alignment of human and parasitic HDACs was prepared in MOE and edited with ESPript tool [68].

### **3.3. Molecular Docking**

Ligands were prepared for docking in MOE in the following way. Three-dimensional ligand structures were generated from simplified molecular-input line-entry system (SMILES) to get random initial ligand position. Different protonation states, tautomers and stereoisomers were prepared in MOE. Hydroxamic acid groups were used in uncharged form. Conformational search was carried out using Low Mode MD sampling within energy window 5 kcal/mol with a minimum root-mean-square deviation (RMSD) of atomic positions 0.5-1.0 Å. This procedure yielded a reasonable number of unbiased low-energy starting conformations.

Structures of relevant proteins were either downloaded from RCSB PDB or homology modelled as described before. They were prepared for docking using Protein Preparation Wizard in Schrödinger suite [69] using the following general scheme. Non-relevant solvent particles were removed. Conserved water molecules located near the catalytic zinc ion were kept in the crystal structures or added to the homology models to be further used for docking if needed. Hydrogens

and missing amino acid side chains were added. Protonation states were predicted at pH 7.0 using PROPKA tool and the hydrogen bond network was optimized. In some cases different histidine states were kept for docking. Finally, protein structures were subjected to restrained energy minimization using the default parameters (OPLS\_2005 force field [70], maximal RMSD of the atom displacement 0.3 Å).

Molecular docking studies were performed on a Linux cluster. Docking protocols slightly varied depending on the target and ligands. Final settings were selected based on re-docking experiments conducted in order to evaluate and validate the docking protocols in each case. Usually docking was performed using Glide application from Schrödinger suite in the standard precision (SP) mode with metal constraint to the zinc ion, and the docking poses were ranked by Glide SP score. However, sometimes additional constraints were used to obtain the hydroxamic acid chelation of the catalytic zinc ion as observed in co-crystal structures. Alternatively, post-docking filter was applied using Schrödinger script `distance_to_smarts` to select docking poses with the desired hydroxamic acid chelation. In some cases, the docking poses obtained by Glide were rescored with scoring functions implemented in the GOLD docking program [71].

### **3.4. Molecular Dynamics Simulation**

Molecular dynamics (MD) simulation of the generated homology models of parasitic HDACs was carried out using AMBER package [72]. Input files were prepared for simulations with LEaP tool. Proteins were parametrized using the AMBER ff99SB force field [73], whereas ligands were parametrized using the general AMBER force field (GAFF) [74] by Antechamber tool and the catalytic zinc ion was parametrized as described by Hoops et al [75]. The molecular system was neutralized by adding counter ions and solvated in a pre-equilibrated truncated octahedral periodic solvent box of TIP3P water [76] with a buffering distance between the edges of the box and the protein of 8 Å.

Energy minimization of the system was performed in three steps gradually reducing tethering on atoms. In the first step positional restraints with a force constant of  $10 \text{ kcal mol}^{-1} \text{ \AA}^{-2}$  were applied to the protein, zinc ion and ligand atoms. In the second step, the protein backbone, zinc ion, ligand atoms and hydroxamic acid group coordinating residues were restrained with the same force constant. At the third step weak restraints with a force constant of  $1 \text{ kcal mol}^{-1} \text{ \AA}^{-2}$  were applied to the heavy atoms of the hydroxamic acid group coordinating residues. In each minimization step

the steepest descent method was applied for the first 500 iterations and the conjugated gradient method for the next 2500 iterations. After minimization, the system was heated from 0 to 300 K under constant volume for 50 ps and relaxed under constant pressure and temperature for another 50 ps keeping all protein and ligand atoms restrained as in the first minimization step. Afterwards, the system was equilibrated in three steps 50 ps each gradually reducing restraints in the same way as during minimization. The equilibrated system was subjected to a 10 ns production MD run without application of restraints. A nonbonded cut-off of 10 Å was used in each step except the production MD, where it was set to 9 Å. To handle long-range electrostatic interactions, the Particle Mesh Ewald method was used [77]. To constraint hydrogen bonds, the SHAKE algorithm was applied [78]. A time step of 2 fs was set in all MD steps.

### **3.5. Binding Free Energy Calculation**

Binding free energy of the docked human HDAC6-inhibitor complexes was calculated using molecular mechanics energies combined with the generalized Born and accessible surface area implicit solvation (MM-GBSA) approach in MOE. The MMFF94 force field [79] was set. Protein heavy atoms were tethered with a force constant of 100 kcal mol<sup>-1</sup> Å<sup>-1</sup>, while ligands inside the binding pocket were minimized until a gradient of 0.05 kcal/mol was reached.

For SmHDAC8-inhibitor complexes the AMBER12EHT force field [72, 80] implemented in MOE and GBSA continuum solvation model were used. Protonate3D tool was applied to fix partial charges according to the used force field followed by a short minimization. Protein-ligand complexes were minimized and the binding free energy for all docking poses of ligands was calculated with an in-house script. Protein heavy atoms were tethered during complex minimization with a deviation of 0.5 Å (force constant (3/2) kT/(0.5)<sup>2</sup>).

### **3.6. Virtual Screening**

Virtual screening on SmHDAC8 was carried out in several steps. The ZINC drug-like database [81] containing 15 million entries was filtered to retrieve ligands with known ZBGs (hydroxamic acids, anilinobenzamides, thiazole sulfonamides). Around 5000 chemical structures fulfilling the search query were collected. All of them were docked to the homology model of SmHDAC8, which was generated using human HDAC8 as a template and following general workflow given

above with additional loop modeling in MODELLER. Docking settings were tested by re-docking the inhibitors co-crystallized with human HDAC8 into the SmHDAC8 homology model. Docking with Glide program, as described previously, was reproducing zinc ion coordination in the top-ranked docking solutions and it was chosen for virtual screening. The ligand conformational search step was omitted to reduce computational costs.

The obtained docking poses were rescored in GOLD docking program using the different implemented scoring functions (GoldScore, ChemScore, ASP, ChemPLP). The top-ranked solutions of Glide and GOLD scoring were considered for further analysis. Docking poses were additionally inspected in MOE to confirm their interaction with the catalytic zinc ion. Based on the listed criteria and commercial availability, 75 compounds were selected and purchased for further *in vitro* testing.

### **3.7. *In vitro* Testing**

The inhibitory activity of the compounds against HDACs was evaluated in the research group of Prof. Dr. Manfred Jung in Freiburg (Germany) using three types of assays. Pre-testing of SmHDAC8 inhibition was carried out with trifluoroacetylated substrate Z(Tfa)Lys-AMC (ZMTFAL). Testing was performed in 96-half-well plates with a reaction mixture containing 25  $\mu\text{M}$  of the substrate, 10  $\mu\text{L}$  SmHDAC8 preparation and 2.5  $\mu\text{L}$  of the inhibitor in varying concentrations. After 90 min of incubation, a trypsin solution as developing agent was added. The activity of the compounds against human HDAC8 and SmHDAC8 was evaluated using commercial HDAC8 Fluorimetric Drug Discovery Kit (Fluor de Lys(R)-HDAC8, BML-KI178) from Enzo Life Sciences following the manufacturer's instructions. The enzyme was incubated for 90 min with a substrate concentration of 50  $\mu\text{M}$  and increasing concentrations of the inhibitors. Subsequently, 50  $\mu\text{L}$  of Developer II (BML-KI176) was added and the mixture was further incubated for 45 min. The inhibition of HDAC1, HDAC3 and HDAC6 was measured using a procedure with Z(Ac)Lys-AMC (ZMAL) as the substrate. The enzyme was incubated for 90 min with a substrate (10.5  $\mu\text{M}$ ) and the test compound. Afterwards, trypsin was added and the mixture was incubated for another 20 min. Fluorescence intensity in all three assays was measured with an excitation wavelength set at 390 nm and an emission detection set at 460 nm.

The antiparasitic activity of the compounds against *S. mansoni* was determined in the research group of Prof. Dr. Raymond J. Pierce in Lille (France). Briefly, the screening assay to determine

the effects of SmHDAC8 inhibitors on the viability of *S. mansoni* schistosomula was carried out in the following way. A schistosomula suspension was prepared and incubated for 3 h. Inhibitor solutions were added to schistosomula suspension in the 96-well plates. After inhibitor exposure of 48 h, resazurin (Alamar Blue) solution was added to each well and 24 h later, the fluorescence intensity of the resorufin product was measured at an excitation wavelength of 530 nm and an emission wavelength of 590 nm. The EC<sub>50</sub> was measured using the same assay with different concentrations of the compound. The effect of SmHDAC8 inhibitors on the viability of schistosomula was tested more detailed by a microscopy-based assay. Schistosomula were incubated for 5 days in six-well plates with different concentrations of the inhibitors. Culture medium was refreshed every day. A minimum of 300 schistosomula was observed by microscopic examination each day taking into account three criteria: absence of motility, tegument defects and granular appearance. The percentage of the remaining viable larvae was calculated. The stability of adult worm pairs and egg laying were also evaluated. Ten worm pairs were placed in each well of a six-well culture plate. Worms were maintained in culture for 5 days before the addition of SmHDAC8 inhibitor solution. The number of pairs remaining together was determined each day by microscopic examination. The eggs were recovered and counted under the microscope.

The inhibition of LpxC and antibacterial activity by the compounds was assayed in the research group of Prof. Dr. Ralph Holl in Münster (Germany). Shortly, the wells in a 96-well fluorescence microplate were filled with buffer (pH 6.0) containing UDP-3-O-[(R)-3-hydroxymyristoyl]-N-acetylglucosamine, dithiothreitol and Brij 35. Inhibitors solutions were assayed over a range starting from 0.2 nM up to 200 µM. Purified LpxC was added and the microplate was incubated for 30 min. The biochemical reaction was stopped by addition of sodium hydroxide solution. The reaction mixture was further incubated for 15 min and neutralized with acetic acid. The deacetylated reaction product UDP-3-O-[(R)-3-hydroxymyristoyl]glucosamine was converted into a fluorescing isoindole by addition of *o*-phthaldialdehyde-2-mercaptoethanol in borax<sup>34</sup> and detected by a plate reader at 340 nm excitation and 460 nm emission wavelengths. The antibacterial activity of the synthesized LpxC inhibitors was evaluated by agar disc diffusion assays. Liquid cultures of *E. coli* BL21 (DE3) and the antibiotic resistant strain *E. coli* D2230 were grown overnight in lysogeny broth. The overnight cell suspension was spread evenly onto lysogeny broth agar petri dishes. A solution of tested compound was applied onto circular filter paper. The petri dishes were incubated overnight and the diameter of the zone of growth inhibition was measured for each compound. Minimum inhibitory concentration values of the compounds were determined by microdilution method. *E. coli* BL21 (DE3) and *E. coli* D22 were grown overnight. The overnight suspension was diluted in fresh lysogeny broth and dispensed to each

well of a 96-well plate. Solutions of the tested compounds were added and the plates were incubated for 20 h. The lowest concentration at which no visible growth of bacteria could be observed was taken as a minimum inhibitory concentration.

For further details or other applied experimental methods please refer to the manuscripts provided in the Appendix 9.2.



## 4. Results and Discussion

Abstracts of eleven manuscripts are presented in this chapter. The full texts of the manuscripts are given in the Appendix 9.2.

### 4.1. Discovery of Inhibitors of *Schistosoma Mansoni* HDAC8 by Combining Homology Modeling, Virtual Screening and *In Vitro* Validation

Kannan S, **Melesina J**, Hauser AT, Chakrabarti A, Heimburg T, Schmidtkunz K, Walter A, Marek M, Pierce RJ, Romier C, Jung M, Sippl W.

J Chem Inf Model, 54, 3005-19, 2014. doi: 10.1021/ci5004653.

Schistosomiasis, caused by *S. mansoni*, is a tropical disease that affects over 200 million people worldwide. A novel approach for targeting eukaryotic parasites is to tackle their dynamic epigenetic machinery that is necessary for the extensive phenotypic changes during their life cycle. We recently identified *S. mansoni* histone deacetylase 8 (SmHDAC8) as a potential target for antiparasitic therapy. Here we present results from a virtual screening campaign on SmHDAC8. Besides hydroxamates, several sulfonamide-thiazole derivatives were identified by a target-based virtual screening using a homology model of SmHDAC8. In vitro testing of 75 compounds identified 8 hydroxamates as potent and lead-like inhibitors of the parasitic HDAC8. Solving of the crystal structure of SmHDAC8 with two of the virtual screening hits confirmed the predicted binding mode.

## 4.2. Molecular Basis for the Antiparasitic Activity of a Mercaptoacetamide Derivative that Inhibits Histone Deacetylase 8 from the Human Pathogen *Schistosoma mansoni*

Stolfa DA, Marek M, Lancelot J, Hauser AT, Walter A, Leproult E, **Melesina J**, Rumpf T, Wurtz JM, Cavarelli J, Sippl W, Pierce RJ, Romier C, Jung M.

J Mol Biol, 426, 3442-53, 2014. doi: 10.1016/j.jmb.2014.03.007.

Schistosomiasis, caused by the parasitic flatworm *Schistosoma mansoni* and related species, is a tropical disease that affects over 200 million people worldwide. A new approach for targeting eukaryotic parasites is to tackle their dynamic epigenetic machinery that is necessary for the extensive phenotypic changes during the life cycle of the parasite. Recently, we identified *S. mansoni* histone deacetylase 8 (SmHDAC8) as a potential target for antiparasitic therapy. Here, we present results on the investigations of a focused set of HDAC (histone deacetylase) inhibitors on SmHDAC8. Besides several active hydroxamates, we identified a thiol-based inhibitor that inhibited SmHDAC8 activity in the micromolar range with unexpected selectivity over the human isotype, which has not been observed so far. The crystal structure of SmHDAC8 complexed with the thiol derivative revealed that the inhibitor is accommodated in the catalytic pocket, where it interacts with both the catalytic zinc ion and the essential catalytic tyrosine (Y341) residue via its mercaptoacetamide warhead. To our knowledge, this is the first complex crystal structure of any HDAC inhibited by a mercaptoacetamide inhibitor, and therefore, this finding offers a rationale for further improvement. Finally, an ester prodrug of the thiol HDAC inhibitor exhibited antiparasitic activity on cultured schistosomes in a dose-dependent manner.

### 4.3. Structure-Based Design and Synthesis of Novel Inhibitors Targeting HDAC8 from *Schistosoma mansoni* for the Treatment of Schistosomiasis

Heimburg T, Chakrabarti A, Lancelot J, Marek M, **Melesina J**, Hauser AT, Shaik TB, Duclaud S, Robaa D, Erdmann F, Schmidt M, Romier C, Pierce RJ, Jung M, Sippl W.

J Med Chem, 59, 2423-35, 2016. doi: 10.1021/acs.jmedchem.5b01478.

Schistosomiasis is a major neglected parasitic disease that affects more than 265 million people worldwide and for which the control strategy consists of mass treatment with the only available drug, praziquantel. In this study, a series of new benzohydroxamates were prepared as potent inhibitors of *Schistosoma mansoni* histone deacetylase 8 (SmHDAC8). Crystallographic analysis provided insights into the inhibition mode of SmHDAC8 activity by these 3-amidobenzohydroxamates. The newly designed inhibitors were evaluated in screens for enzyme inhibitory activity against schistosome and human HDACs. Twenty-seven compounds were found to be active in the nanomolar range, and some of them showed selectivity toward SmHDAC8 over the major human HDACs (1 and 6). The active benzohydroxamates were additionally screened for lethality against the schistosome larval stage using a fluorescence-based assay. Four of these showed significant dose-dependent killing of the schistosome larvae and markedly impaired egg laying of adult worm pairs maintained in culture.

## 4.4. Isophthalic Acid-Based HDAC Inhibitors as Potent Inhibitors of HDAC8 from *Schistosoma mansoni*

Stenzel K, Chakrabarti A, **Melesina J**, Hansen FK, Lancelot J, Herkenhöner S, Lungerich B, Marek M, Romier C, Pierce RJ, Sippl W, Jung M, Kurz T.

Arch Pharm (Weinheim), 350(8), 2017. doi: 10.1002/ardp.201700096.

*Schistosoma mansoni* histone deacetylase 8 (SmHDAC8) has been recently identified as a new potential target for the treatment of schistosomiasis. A series of newly designed and synthesized alkoxyamide-based and hydrazide-based HDAC inhibitors were tested for inhibitory activity against SmHDAC8 and human HDACs 1, 6, and 8. The front runner compounds showed submicromolar activity against SmHDAC8 and modest preference for SmHDAC8 over its human orthologue hHDAC8. Docking studies provided insights into the putative binding mode in SmHDAC8 and allowed rationalization of the observed selectivity profile.

## 4.5. Homology Modeling of Parasite Histone Deacetylases to Guide the Structure-Based Design of Selective Inhibitors

Melesina J, Robaa D, Pierce RJ, Romier C, Sippl W.

J Mol Graph Model, 62, 342-61, 2015. doi: 10.1016/j.jmglm.2015.10.006.

Histone deacetylases (HDACs) are promising epigenetic targets for the treatment of various diseases, including cancer and neurodegenerative disorders. There is evidence that they can also be addressed to treat parasitic infections. Recently, the first X-ray structure of a parasite HDAC was published, *Schistosoma mansoni* HDAC8, giving structural insights into its inhibition. However, most of the targets from parasites of interest still lack this structural information. Therefore, we prepared homology models of relevant parasitic HDACs and compared them to human and *S. mansoni* HDACs. The information about known *S. mansoni* HDAC8 inhibitors and compounds that affect the growth of *Trypanosoma*, *Leishmania* and *Plasmodium* species was used to validate the models by docking and molecular dynamics studies. Our results provide analysis of structural features of parasitic HDACs and should be helpful for selecting promising candidates for biological testing and for structure-based optimization of parasite-specific inhibitors.

## 4.6. Evolutionary Relationships among Protein Lysine Deacetylases of Parasites Causing Neglected Diseases

Scholte LLS, Mourão MM, Pais FS, **Melesina J**, Robaa D, Volpini AC, Sippl W, Pierce RJ, Oliveira G, Nahum LA.

Infect Genet Evol. 53, 175-188, 2017. doi: 10.1016/j.meegid.2017.05.011.

The availability of the genomic data of diverse parasites provides an opportunity to identify new drug candidates against neglected tropical diseases affecting people worldwide. Histone modifying enzymes (HMEs) are potential candidates since they play key roles in the regulation of chromatin modifications, thus globally regulating gene expression. Furthermore, aberrant epigenetic states are often associated with human diseases, leading to great interest in HMEs as therapeutic targets. Our work focused on two families of protein lysine deacetylases (HDACs and sirtuins). First, we identified potential homologues in the predicted proteomes of selected taxa by using hidden Markov model profiles. Then, we reconstructed the evolutionary relationships of protein sequences by Bayesian inference and maximum likelihood method. In addition, we constructed homology models for five parasite HDACs to provide information for experimental validation and structure-based optimization of inhibitors. Our results showed that parasite genomes code for diverse HDACs and sirtuins. The evolutionary pattern of protein deacetylases with additional experimental data points to these enzymes as common drug targets among parasites. This work has improved the functional annotation of approximately 63% HDACs and 51% sirtuins in the selected taxa providing insights for experimental design. Homology models pointed out structural conservation and differences among parasite and human homologues and highlight potential candidates for further inhibitor development. Some of these parasite proteins are undergoing RNA interference or knockout analyses to validate the function of their corresponding genes. In the future, we will investigate the main functions performed by these proteins, related phenotypes, and their potential as therapeutic targets.

## 4.7. Targeting Histone Deacetylase 8 as a Therapeutic Approach to Cancer and Neurodegenerative Diseases

Chakrabarti A, **Melesina J**, Kolbinger FR, Oehme I, Senger J, Witt O, Sippl W, Jung M.

Future Med Chem, 8, 1609-34, 2016. doi: 10.4155/fmc-2016-0117.

Histone deacetylase 8 (HDAC8), a unique class I zinc-dependent HDAC, is an emerging target in cancer and other diseases. Its substrate repertoire extends beyond histones to many nonhistone proteins. Besides being a deacetylase, HDAC8 also mediates signaling via scaffolding functions. Aberrant expression or deregulated interactions with transcription factors are critical in HDAC8-dependent cancers. Many potent HDAC8-selective inhibitors with cellular activity and anticancer effects have been reported. We present HDAC8 as a druggable target and discuss inhibitors of different chemical scaffolds with cellular effects. Furthermore, we review HDAC8 activators that revert activity of mutant enzymes. Isotype-selective HDAC8 targeting in patients with HDAC8-relevant cancers is challenging, however, is promising to avoid adverse side effects as observed with pan-HDAC inhibitors.

## 4.8. Synthesis and Biological Investigation of Oxazole Hydroxamates as Highly Selective Histone Deacetylase 6 (HDAC6) Inhibitors

Senger J, **Melesina J**, Marek M, Romier C, Oehme I, Witt O, Sippl W, Jung M.

J Med Chem, 59, 1545-55, 2016. doi: 10.1021/acs.jmedchem.5b01493.

Histone deacetylase 6 (HDAC6) catalyzes the removal of an acetyl group from lysine residues of several non-histone proteins. Here we report the preparation of thiazole-, oxazole-, and oxadiazole-containing biarylhydroxamic acids by a short synthetic procedure. We identified them as selective HDAC6 inhibitors by investigating the inhibition of recombinant HDAC enzymes and the protein acetylation in cells by Western blotting (tubulin vs histone acetylation). The most active compounds exhibited nanomolar potency and high selectivity for HDAC6. For example, an oxazole hydroxamate inhibits HDAC6 with an  $IC_{50}$  of 59 nM and has a selectivity index of >200 against HDAC1 and HDAC8. This is the first report showing that the nature of a heterocycle directly connected to a zinc binding group (ZBG) can be used to modulate subtype selectivity and potency for HDAC6 inhibitors to such an extent. We rationalize the high potency and selectivity of the oxazoles by molecular modeling and docking.



## 4.9. 2-Benzazolyl-4-piperazin-1-ylsulfonylbenzenecarbohydroxamic Acids as Novel Histone Deacetylase-6 Inhibitors with Antiproliferative Activity

Wang L, Kofler M, Brosch G, **Melesina J**, Sippl W, Martinez ED, Easmon J.

PLoS One, 10, e0134556, 2015. doi: 10.1371/journal.pone.0134556.

We have screened our compound collection in an established cell based assay that measures the derepression of an epigenetically silenced transgene, the locus derepression assay. The screen led to the identification of 4-[4-(1-methylbenzimidazol-2-yl)piperazin-1-yl]sulfonylbenzenecarbohydroxamic acid (**9b**) as an active which was found to inhibit HDAC1. In initial structure activity relationships study, the 1-methylbenzimidazole ring was replaced by the isosteric heterocycles benzimidazole, benzoxazole, and benzothiazole and the position of the hydroxamic acid substituent on the phenyl ring was varied. Whereas compounds bearing a *para* substituted hydroxamic acid (**9a-d**) were active HDAC inhibitors, the *meta* substituted analogues (**8a-d**) were appreciably inactive. Compounds **9a-d** selectively inhibited HDAC6 ( $IC_{50} = 0.1-1.0 \mu M$ ) over HDAC1 ( $IC_{50} = 0.9-6 \mu M$ ) and moreover, also selectively inhibited the growth of lung cancer cells vs. patient matched normal cells. The compounds induce a cell cycle arrest in the S-phase while induction of apoptosis is negligible as compared to controls. Molecular modeling studies uncovered that the MM-GBSA energy for interaction of **9a-d** with HDAC6 was higher than for HDAC1 providing structural rationale for the HDAC6 selectivity.

## 4.10. Synthesis, Biological Evaluation and Molecular Docking Studies of Benzyloxyacetohydroxamic Acids as LpxC Inhibitors

Szermerski M, Melesina J, Wichapong K, Löppenber M, Jose J, Sippl W, Holl R.

Bioorg Med Chem, 22, 1016-28, 2014. doi: 10.1016/j.bmc.2013.12.057.

The inhibition of the UDP-3-O-[(R)-3-hydroxymyristoyl]-N-acetylglucosamine deacetylase (LpxC) represents a promising strategy to combat infections caused by multidrug-resistant Gram-negative bacteria. In order to elucidate the functional groups being important for the inhibition of LpxC, the structure of our previously reported hydroxamic acid **4** should be systematically varied. Therefore, a series of benzyloxyacetohydroxamic acids was prepared, of which the diphenylacetylene derivatives **28** ( $K_i = 95$  nM) and **21** ( $K_i = 66$  nM) were the most potent inhibitors of *Escherichia coli* LpxC. These compounds could be synthesized in a stereoselective manner employing a Sharpless asymmetric dihydroxylation and a Sonogashira coupling in the key steps. The obtained structure-activity relationships could be rationalized by molecular docking studies.

## 4.11. Synthesis and Biological Evaluation of Enantiomerically Pure Glyceric Acid Derivatives as LpxC Inhibitors

Tangherlini G, Torregrossa T, Agoglitta O, Köhler J, Melesina J, Sippl W, Holl R.

Bioorg Med Chem, 24, 1032-44, 2016. doi: 10.1016/j.bmc.2016.01.029.

Inhibitors of the UDP-3-O-[(*R*)-3-hydroxymyristoyl]-*N*-acetylglucosamine deacetylase (LpxC) represent a promising class of novel antibiotics, selectively combating Gram-negative bacteria. In order to elucidate the impact of the hydroxymethyl groups of diol (*S,S*)-**4** on the inhibitory activity against LpxC, glyceric acid ethers (*R*)-**7a**, (*S*)-**7a**, (*R*)-**7b**, and (*S*)-**7b**, lacking the hydroxymethyl group in benzylic position, were synthesized. The compounds were obtained in enantiomerically pure form by a chiral pool synthesis and a lipase-catalyzed enantioselective desymmetrization, respectively. The enantiomeric hydroxamic acids (*R*)-**7b** ( $K_i = 230$  nM) and (*S*)-**7b** ( $K_i = 390$  nM) show promising enzyme inhibition. However, their inhibitory activities do not substantially differ from each other leading to a low eudismic ratio. Generally, the synthesized glyceric acid derivatives **7** show antibacterial activities against two *Escherichia coli* strains exceeding the ones of their respective regioisomers **6**.

## 5. Conclusions

Zinc-dependent enzymes are investigated as drug targets due to their multiple functions *in vivo*. Specifically, HDACs and LpxCs, which are the focus of this work, are targeted for the treatment of cancer, parasitic diseases and bacterial infections. Development of small molecule inhibitors against these enzymes is a promising approach to search for novel drug candidates. However, to achieve a reasonable level of efficacy and safety, potent inhibition of the target enzyme *in vitro* is not sufficient. Also the physicochemical properties and selectivity have to be adjusted to reach the desired protein in the affected organism and to exclusively target it. Therefore, the search for the optimal inhibitor demands interdisciplinary cooperation and is time-consuming. To speed up the research, a rational computer-aided design of inhibitors can be helpful.

The results of our efforts to identify and develop inhibitors of zinc-dependent enzymes using computer-assisted approaches are presented in the previous chapter in eleven manuscripts. The first seven manuscripts are devoted to the antiparasitic target SmHDAC8 and other parasitic HDACs, the next two manuscripts to the anticancer target HDAC6 and the last two manuscripts to the antibacterial target LpxC. In this last chapter the results are summarized and the main achievements are highlighted. Additionally, general conclusions regarding inhibitor development and application of computational methods are made, strategies for future research in this field are recommended.

### 5.1. Hit Identification for SmHDAC8

A structure-based virtual screening was carried out in order to identify first hits for the newly-validated antiparasitic target SmHDAC8. A database of approximately 15 million chemical structures was filtered to retrieve entries with known ZBGs. Around 5000 candidate zinc binders were docked to a homology model of SmHDAC8 built on human HDAC8 as a template. Based on docking scores and visual inspection, 75 compounds with hydroxamic acid, thiazole sulfonamide and anilinobenzamide ZBGs were selected and purchased for biological screening on SmHDAC8. Among them 26 active compounds were found. For the 6 most potent hits the  $IC_{50}$  values were determined, which ranged between 1 and 6  $\mu$ M. These hits were all hydroxamic acids and included one known human HDAC inhibitor tubastatin A as well as five novel HDAC inhibitors T5971079, J1038 (T5979345), T6072858, Z59184147 and K783-3816 (Fig. 7a). Besides the novel structure,

these five inhibitors also exhibited better selectivity towards HDAC8 isoform over HDAC1 and HDAC6 in comparison to known tested HDAC inhibitors vorinostat, M344 and tubastatin A. Unfortunately, none of the found hits was selective towards SmHDAC8 over human HDAC8. (Manuscript 4.1)

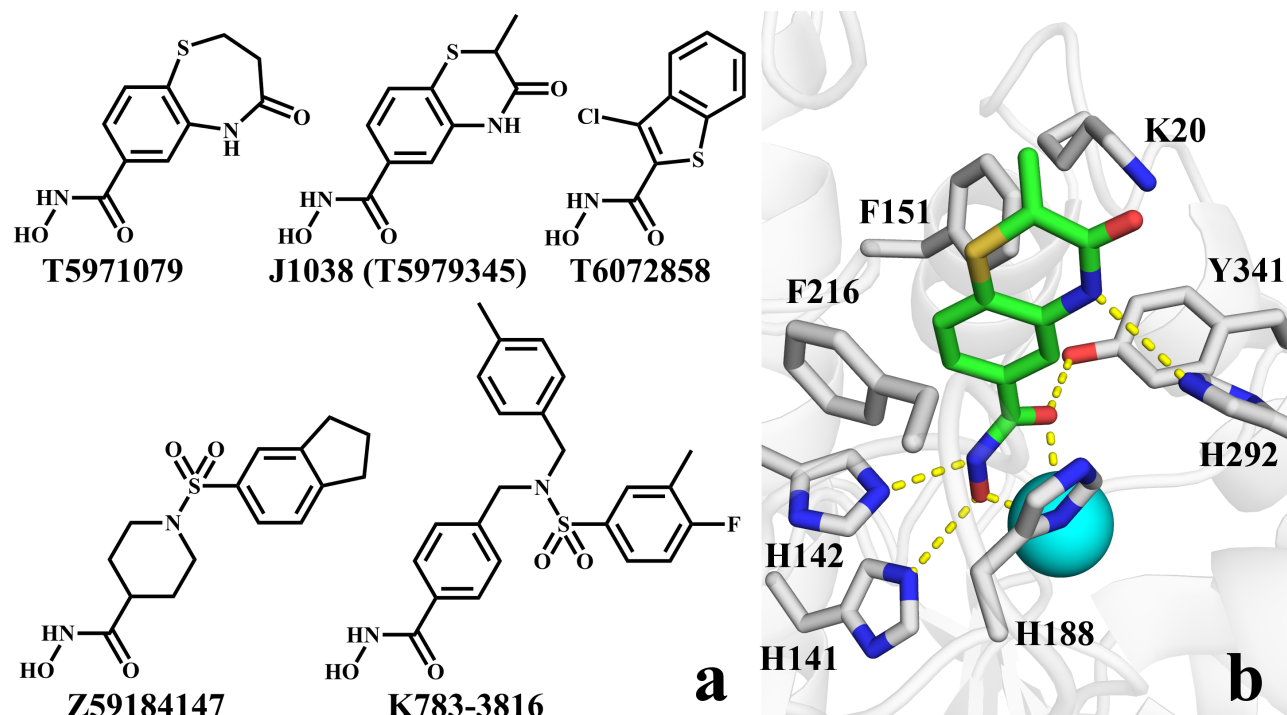


**Figure 7.** Novel SmHDAC8 inhibitors identified with a structure-based virtual screening approach (a) and J1038 binding mode (PDB ID 4BZ8) (b)

In parallel, a focused library of 15 known and putative HDAC inhibitors was screened *in vitro* against SmHDAC8. All 10 screened hydroxamic acids inhibited SmHDAC8 in a low micromolar range, but again none of them showed selectivity towards SmHDAC8 over human HDAC8. The inhibitors which had non-hydroxamate ZBGs (carboxylic acid, prodrug of mercaptoacetamide, epoxide and amino acid derivative) were inactive except the vorinostat analog with a mercaptoacetamide ZBG. This compound was four times more active on SmHDAC8 than on human HDAC8, however, it was only weakly active with  $IC_{50}$  of 50  $\mu$ M. In order to rationalize the observed experimental data, docking studies were carried out. Interestingly, docking scores were in agreement with biological data and allowed to build a predictive computational model, which could be used for optimization of the retrieved hits. (Manuscript 4.2)

This model, however, was not utilized, because the hit selected for further development, belonged to the list obtained from the aforementioned virtual screening. J1038 was chosen for further

optimization due to its optimal activity and selectivity profile together with its small fragment-like size and a novel structure. Furthermore, its crystal structure with the target protein (PDB ID 4BZ8) has been obtained and used for structure-based computer-aided drug design (Fig. 7b).

## 5.2. Optimization of SmHDAC8 Inhibitors

The crystal structure of SmHDAC8 with the virtual screening hit J1038 showed that the amide group of the inhibitor is making a hydrogen bond with the unique SmHDAC8 residue H292 (Fig. 7b). Taking this into account, an open-ring  $\Gamma$ -shaped analogue **1** (Fig. 8a) maintaining this hydrogen bond and targeting the HDAC8-specific side pocket was designed. Its crystal structure with SmHDAC8 (PDB ID 5FUE) confirmed the expected binding mode (Fig. 8b) and added  $\Gamma$ -shape to the list of I-, J- and L-shapes of HDAC inhibitors discussed in the Introduction (Fig. 6). Additionally, an unexpected hydrogen bond between the carbonyl group of the amide linker and K20 was formed due to rearrangement of the binding pocket residues, namely a SmHDAC8-specific castling between F151 and K20. This additional hydrogen bond further stabilized the observed binding mode of compound **1**. (Manuscript 4.3)

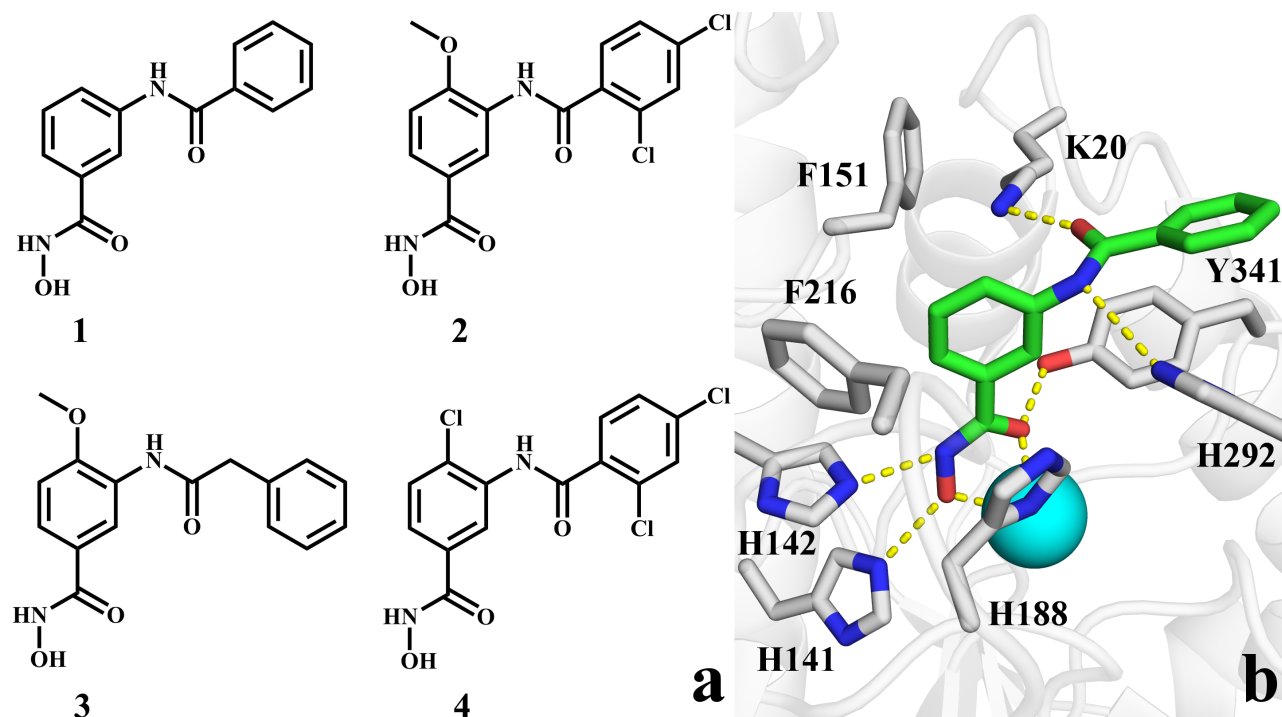


**Figure 8.** Optimized SmHDAC8 inhibitors designed using computer-based methods (a) and binding mode of compound **1** (PDB ID 5FUE) (b)

A library of various  $\Gamma$ -shaped 3-substituted benzohydroxamic acids was generated and docked to SmHDAC8 and human HDACs binding pockets. Based on computational studies, the most promising structures were recommended for further synthesis and biological testing. Around 50 compounds were prepared and their inhibitory activity on SmHDAC8, human HDAC8, HDAC1 and HDAC6 was measured. The determined  $IC_{50}$  values on SmHDAC8 ranged between 0.1 and 9  $\mu$ M. In contrast, the  $IC_{50}$  values on human HDAC1 were much higher, since the inhibitors did not fit into the relatively narrow substrate binding channel of this isoform as suggested by docking studies. Most inhibitors were also less active on HDAC6, nevertheless, they demonstrated reasonable docking poses. This is more difficult to explain due to the interplay between the two deacetylase domains of this isoform. Surprisingly, the activity on human HDAC8 was on the same level or higher for most inhibitors despite the loss of the hydrogen bond to the unique SmHDAC8 H292 residue substituted by M274 in human HDAC8. According to the docking studies, this protein-ligand interaction could be compensated by a similar hydrogen bond with a conserved water molecule situated in close proximity. Nevertheless, three 3-amidobenzohydroxamic acids (2-4, Fig. 8a) with  $IC_{50}$  100-200 nM were significantly selective over human HDAC8 (3-6 fold), as well as HDAC1 (more than 100 fold) and HDAC6 (4-28 fold). Docking poses explained that these compounds could probably gain additional van der Waals interactions deep in the side pocket, which were more favorable in SmHDAC8. Additionally, a substituent at position 4 stabilized the bioactive conformation in SmHDAC8, but not in human HDAC8. Our results showed that even with a single amino acid difference in the binding pocket of SmHDAC8 and human HDAC8 it was possible to obtain selective inhibitors. (Manuscripts 4.3 and 4.4)

Furthermore, 32 benzohydroxamic acids were tested for their antiparasitic activity on *S. mansoni* schistosomula maintained in culture. The most active compound 3-biphenyl-4-methoxybenzohydroxamic acid was lethal on schistosomula with  $EC_{50}$  16  $\mu$ M. Thus, it was confirmed that this compound is not only able to act on the target enzyme, but also to penetrate the parasitic organism and induce its death. (Manuscripts 4.3 and 4.4)

### **5.3. Assisting Target Validation of Parasitic HDACs**

Successful development of parasite-killing SmHDAC8 inhibitors inspired us to search for other suitable targets. With the help of computational methods, 30 models of parasitic HDACs were generated and analyzed. First, homology models of SmHDAC8 orthologues in other platyhelminth species (*Schistosoma haematobium*, *S. japonicum*, *Clonorchis sinensis*, *Echinococcus*

*multilocularis*, *E. granulosus*, *Taenia solium* and *Hymenolepis microstoma*) were examined. Analysis revealed that they all share parasite-specific SmHDAC8 binding pocket features: histidine residue H292 and flipping of F151 side chain. Therefore, the developed SmHDAC8 inhibitors are likely to act as pan-platyhelminth HDAC8 inhibitors. Secondly, homology models of *S. mansoni*, *Trypanosoma brucei*, *T. cruzi*, *Leishmania braziliensis*, *L. major* and *Plasmodium falciparum* HDACs were built and compared to human HDACs in order to identify features, which could be targeted by rational inhibitor design. Unique binding pocket amino acid residues were identified and highlighted for each protein model. Furthermore, the formation of the side pocket and the foot pocket was predicted for various parasitic HDAC isoforms and inhibitor structures were suggested according to visual inspection and docking studies. These findings can be considered when choosing antiparasitic targets for further validation and to guide the design of selective inhibitors. (Manuscripts 4.5-4.7)

## 5.4. Optimization of Human HDAC6 Inhibitors

Two series of human HDAC6 inhibitors have been developed in the research laboratories of M. Jung and J. Easmon. The obtained biological activity data required rationalization, therefore, molecular docking and binding free energy calculations were applied to pave the way for future optimization of the inhibitors. For instance, it was not clear why a series of hydroxamic acids with an oxazole linker exhibited high potency and selectivity towards HDAC6, while their thiazole analogs were significantly less active. According to the docking poses, the larger size of the sulfur atom was changing the orientation of the ligand and pushing the hydrophobic groups further away from the lipophilic residues F566 and F520. This resulted in less favorable interactions and a decrease in inhibitory activity. For a second series of inhibitors binding free energy calculations predicted that the investigated compounds will have better activity on HDAC6 in comparison to HDAC1, which was later confirmed experimentally. (Manuscripts 4.8 and 4.9)

## 5.5. Optimization of Bacterial LpxC Inhibitors

Finally, curious biological data, which also required explanation, has been obtained in the research group of R. Holl for two series of LpxC inhibitors. In the first set of compounds, some of the representatives lacked inhibitory activity. Predicted binding poses showed, that these compounds were losing important interactions with residues in the LpxC binding pocket in comparison to



active compounds. The docking scores were able to discriminate between active and inactive compounds and strongly correlated with bioactivity values. In the second set of compounds, *R*- and *S*- stereoisomers either showed similar activities, or differed 65-290 fold. An explanation for this unusual structure-activity relationship was again provided by the docking poses. It turned out, that only the highly active stereoisomers were substituting the conserved water molecule in the binding pocket and mimicking its interactions. This probably resulted in the gain of entropy from releasing this water into the solvent and the observed activity cliff. (Manuscripts 4.10 and 4.11)

## 5.6. General Conclusions

To conclude, presented case studies demonstrate that computational methods are especially useful for the development of inhibitors of zinc-dependent enzymes. Specifically, due to a distinct feature of such inhibitors - the presence of the ZBG, which offers a number of advantages. Firstly, binding modes of inhibitors are well predictable by molecular docking, because of the anchoring to the metal ion. Secondly, known or putative ZBGs can be used as filters during virtual screening to narrow the chemical space of potential inhibitors. On the other hand, development of inhibitors bearing ZBGs is also associated with some problems. In particular, metal ions have to be correctly parametrized due to their different nature of interactions in comparison to mostly occurring covalent and non-covalent bonds. Furthermore, the same ZBG can sometimes interact with multiple metalloproteins and cause off-target effects, which underlines the importance of selectivity. The selectivity between families of proteins is relatively easy to achieve, but since the members of the same family are highly similar, it might be quite challenging to come up with a subtype-selective compound. Nevertheless, several strategies exist to overcome the selectivity problem. Particularly successful in our case was the design of inhibitors with a novel shape, which allowed them to occupy isoform-specific subpocket. By subsequent computer-aided optimization it was possible to achieve selectivity even between highly similar enzymes with a single amino acid difference in the binding pocket. The applied strategies and protocols are experimentally validated through interdisciplinary collaboration and hopefully will be useful for other projects related to development of metalloenzyme inhibitors.

## 6. References

1. Maret W. Zinc biochemistry: from a single zinc enzyme to a key element of life. *Adv Nutr*. 2013 Jan 1;4(1):82-91.
2. McCall KA, Huang C, Fierke CA. Function and mechanism of zinc metalloenzymes. *J Nutr*. 2000 May;130(5S Suppl):1437S-46S.
3. Bairoch A. The ENZYME database in 2000. *Nucleic Acids Res*. 2000 Jan 1;28(1):304-5.
4. Crabb DW, Matsumoto M, Chang D, You M. Overview of the role of alcohol dehydrogenase and aldehyde dehydrogenase and their variants in the genesis of alcohol-related pathology. *Proc Nutr Soc*. 2004 Feb;63(1):49-63.
5. Palsuledesai CC, Distefano MD. Protein prenylation: enzymes, therapeutics, and biotechnology applications. *ACS Chem Biol*. 2015 Jan 16;10(1):51-62.
6. Haeggström JZ, Tholander F, Wetterholm A. Structure and catalytic mechanisms of leukotriene A4 hydrolase. *Prostaglandins Other Lipid Mediat*. 2007 May;83(3):198-202.
7. Gonzalez-Villalobos RA, Shen XZ, Bernstein EA, Janjulia T, Taylor B, Giani JF, Blackwell WL, Shah KH, Shi PD, Fuchs S, Bernstein KE. Rediscovering ACE: novel insights into the many roles of the angiotensin-converting enzyme. *J Mol Med (Berl)*. 2013 Oct;91(10):1143-54.
8. Hernick M, Fierke CA. Zinc hydrolases: the mechanisms of zinc-dependent deacetylases. *Arch Biochem Biophys*. 2005 Jan 1;433(1):71-84.
9. Supuran CT, Scozzafava A. Carbonic anhydrases as targets for medicinal chemistry. *Bioorg Med Chem*. 2007 Jul 1;15(13):4336-50.
10. Cleasby A, Wonacott A, Skarzynski T, Hubbard RE, Davies GJ, Proudfoot AE, Bernard AR, Payton MA, Wells TN. The X-ray crystal structure of phosphomannose isomerase from *Candida albicans* at 1.7 angstrom resolution. *Nat Struct Biol*. 1996 May;3(5):470-9.
11. St Maurice M, Reinhardt L, Surinya KH, Attwood PV, Wallace JC, Cleland WW, Rayment I. Domain architecture of pyruvate carboxylase, a biotin-dependent multifunctional enzyme. *Science*. 2007 Aug 24;317(5841):1076-9.
12. Benedetti R, Conte M, Altucci L. Targeting histone deacetylases in diseases: where are we? *Antioxid Redox Signal*. 2015 Jul 1;23(1):99-126.
13. Kawai K, Nagata N. Metal-ligand interactions: an analysis of zinc binding groups using the Protein Data Bank. *Eur J Med Chem*. 2012 May;51:271-6.
14. Day JA, Cohen SM. Investigating the selectivity of metalloenzyme inhibitors. *J Med Chem*. 2013 Oct 24;56(20):7997-8007.

15. Haberland M, Montgomery RL, Olson EN. The many roles of histone deacetylases in development and physiology: implications for disease and therapy. *Nat Rev Genet.* 2009 Jan;10(1):32-42. doi: 10.1038/nrg2485.
16. Yoshida M, Kudo N, Kosono S, Ito A. Chemical and structural biology of protein lysine deacetylases. *Proc Jpn Acad Ser B Phys Biol Sci.* 2017;93(5):297-321.
17. Gao L, Cueto MA, Asselbergs F, Atadja P. Cloning and functional characterization of HDAC11, a novel member of the human histone deacetylase family. *J Biol Chem.* 2002 Jul 12;277(28):25748-55.
18. Hai Y, Shinsky SA, Porter NJ, Christianson DW. Histone deacetylase 10 structure and molecular function as a polyamine deacetylase. *Nat Commun.* 2017 May 18;8:15368.
19. McClure JJ, Inks ES, Zhang C, Peterson YK, Li J, Chundru K, Lee B, Buchanan A, Miao S, Chou CJ. Comparison of the deacylase and deacetylase activity of zinc-dependent HDACs. *ACS Chem Biol.* 2017 Jun 16;12(6):1644-1655.
20. Kutil Z, Novakova Z, Meleshin M, Mikesova J, Schutkowski M, Barinka C. Histone deacetylase 11 is a fatty-acid deacylase. *ACS Chem Biol.* 2018 Jan 30.
21. Bradner JE, West N, Grachan ML, Greenberg EF, Haggarty SJ, Warnow T, Mazitschek R. Chemical phylogenetics of histone deacetylases. *Nat Chem Biol.* 2010 Mar;6(3):238-243.
22. Hai Y, Christianson DW. Histone deacetylase 6 structure and molecular basis of catalysis and inhibition. *Nat Chem Biol.* 2016 Sep;12(9):741-7.
23. Schapira M. Structural biology of human metal-dependent histone deacetylases. *Handb Exp Pharmacol.* 2011;206:225-40.
24. Somoza JR, Skene RJ, Katz BA, Mol C, Ho JD, Jennings AJ, Luong C, Arvai A, Buggy JJ, Chi E, Tang J, Sang BC, Verner E, Wynands R, Leahy EM, Dougan DR, Snell G, Navre M, Knuth MW, Swanson RV, McRee DE, Tari LW. Structural snapshots of human HDAC8 provide insights into the class I histone deacetylases. *Structure.* 2004 Jul;12(7):1325-34.
25. Micelli C, Rastelli G. Histone deacetylases: structural determinants of inhibitor selectivity. *Drug Discov Today.* 2015 Jun;20(6):718-735.
26. Eckschlager T, Plch J, Stiborova M, Hrabeta J. Histone deacetylase inhibitors as anticancer drugs. *Int J Mol Sci.* 2017 Jul 1;18(7). pii: E1414.
27. Andrews KT, Haque A, Jones MK. HDAC inhibitors in parasitic diseases. *Immunol Cell Biol.* 2012 Jan;90(1):66-77.
28. Oger F, Dubois F, Caby S, Noël C, Cornette J, Bertin B, Capron M, Pierce RJ. The class I histone deacetylases of the platyhelminth parasite *Schistosoma mansoni*. *Biochem Biophys Res Commun.* 2008 Dec 26;377(4):1079-84.
29. Marek M, Kannan S, Hauser AT, Moraes Mourão M, Caby S, Cura V, Stolfa DA,

- Schmidtkunz K, Lancelot J, Andrade L, Renaud JP, Oliveira G, Sippl W, Jung M, Cavarelli J, Pierce RJ, Romier C. Structural basis for the inhibition of histone deacetylase 8 (HDAC8), a key epigenetic player in the blood fluke *Schistosoma mansoni*. *PLoS Pathog.* 2013;9(9):e1003645.
30. Dubois F, Caby S, Oger F, Cosseau C, Capron M, Grunau C, Dissous C, Pierce RJ. Histone deacetylase inhibitors induce apoptosis, histone hyperacetylation and up-regulation of gene transcription in *Schistosoma mansoni*. *Mol Biochem Parasitol.* 2009 Nov;168(1):7-15.
31. Barb AW, Zhou P. Mechanism and inhibition of LpxC: an essential zinc-dependent deacetylase of bacterial lipid A synthesis. *Curr Pharm Biotechnol.* 2008 Feb;9(1):9-15.
32. Clayton GM, Klein DJ, Rickert KW, Patel SB, Kornienko M, Zugay-Murphy J, Reid JC, Tummala S, Sharma S, Singh SB, Miesel L, Lumb KJ, Soisson SM. Structure of the bacterial deacetylase LpxC bound to the nucleotide reaction product reveals mechanisms of oxyanion stabilization and proton transfer. *J Biol Chem.* 2013 Nov 22;288(47):34073-80.
33. Lee CJ, Liang X, Chen X, Zeng D, Joo SH, Chung HS, Barb AW, Swanson SM, Nicholas RA, Li Y, Toone EJ, Raetz CR, Zhou P. Species-specific and inhibitor-dependent conformations of LpxC: implications for antibiotic design. *Chem Biol.* 2011 Jan 28;18(1):38-47.
34. Onishi HR, Pelak BA, Gerckens LS, Silver LL, Kahan FM, Chen MH, Patchett AA, Galloway SM, Hyland SA, Anderson MS, Raetz CR. Antibacterial agents that inhibit lipid A biosynthesis. *Science.* 1996 Nov 8;274(5289):980-2.
35. Lemaître N, Liang X, Najeeb J, Lee CJ, Titecat M, Leteurtre E, Simonet M, Toone EJ, Zhou P, Sebbane F. Curative treatment of severe Gram-negative bacterial infections by a new class of antibiotics targeting LpxC. *MBio.* 2017 Jul 25;8(4). pii: e00674-17.
36. Kalinin DV, Holl R. Insights into the zinc-dependent deacetylase LpxC: biochemical properties and inhibitor design. *Curr Top Med Chem.* 2016;16(21):2379-430.
37. Shen S, Kozikowski AP. Why hydroxamates may not be the best histone deacetylase inhibitors--what some may have forgotten or would rather forget? *ChemMedChem.* 2016 Jan 5;11(1):15-21.
38. Bottomley MJ, Lo Surdo P, Di Giovine P, Cirillo A, Scarpelli R, Ferrigno F, Jones P, Neddermann P, De Francesco R, Steinkühler C, Gallinari P, Carfi A. Structural and functional analysis of the human HDAC4 catalytic domain reveals a regulatory structural zinc-binding domain. *J Biol Chem.* 2008 Sep 26;283(39):26694-704.
39. Lobera M, Madauss KP, Pohlhaus DT, Wright QG, Trocha M, Schmidt DR, Baloglu E, Trump RP, Head MS, Hofmann GA, Murray-Thompson M, Schwartz B, Chakravorty S, Wu Z, Mander PK, Kruidenier L, Reid RA, Burkhart W, Turunen BJ, Rong JX, Wagner C,

- Moyer MB, Wells C, Hong X, Moore JT, Williams JD, Soler D, Ghosh S, Nolan MA. Selective class IIa histone deacetylase inhibition via a nonchelating zinc-binding group. *Nat Chem Biol.* 2013 May;9(5):319-25.
40. Porter NJ, Christianson DW. Binding of the microbial cyclic tetrapeptide trapoxin A to the class I histone deacetylase HDAC8. *ACS Chem Biol.* 2017 Sep 15;12(9):2281-2286.
41. Whitehead L, Dobler MR, Radetich B, Zhu Y, Atadja PW, Claiborne T, Grob JE, McRiner A, Pancost MR, Patnaik A, Shao W, Shultz M, Tichkule R, Tommasi RA, Vash B, Wang P, Stams T. Human HDAC isoform selectivity achieved via exploitation of the acetate release channel with structurally unique small molecule inhibitors. *Bioorg Med Chem.* 2011 Aug 1;19(15):4626-34.
42. Balasubramanian S, Verner E, Buggy JJ. Isoform-specific histone deacetylase inhibitors: the next step? *Cancer Lett.* 2009 Aug 8;280(2):211-21.
43. Pontiki E, Hadjipavlou-Litina D. Histone deacetylase inhibitors (HDACIs). Structure--activity relationships: history and new QSAR perspectives. *Med Res Rev.* 2012 Jan;32(1):1-165.
44. Lauffer BE, Mintzer R, Fong R, Mukund S, Tam C, Zilberleyb I, Flicke B, Ritscher A, Fedorowicz G, Vallero R, Ortwine DF, Gunzner J, Modrusan Z, Neumann L, Koth CM, Lupardus PJ, Kaminker JS, Heise CE, Steiner P. Histone deacetylase (HDAC) inhibitor kinetic rate constants correlate with cellular histone acetylation but not transcription and cell viability. *J Biol Chem.* 2013 Sep 13;288(37):26926-43.
45. Maolanon AR, Madsen AS, Olsen CA. Innovative strategies for selective inhibition of histone deacetylases. *Cell Chem Biol.* 2016 Jul 21;23(7):759-68.
46. Bürli RW, Luckhurst CA, Aziz O, Matthews KL, Yates D, Lyons KA, Beconi M, McAllister G, Breccia P, Stott AJ, Penrose SD, Wall M, Lamers M, Leonard P, Müller I, Richardson CM, Jarvis R, Stones L, Hughes S, Wishart G, Haughan AF, O'Connell C, Mead T, McNeil H, Vann J, Mangette J, Maillard M, Beaumont V, Munoz-Sanjuan I, Dominguez C. Design, synthesis, and biological evaluation of potent and selective class IIa histone deacetylase (HDAC) inhibitors as a potential therapy for Huntington's disease. *J Med Chem.* 2013 Dec 27;56(24):9934-54.
47. Piizzi G, Parker DT, Peng Y, Dobler M, Patnaik A, Wattanasin S, Liu E, Lenoir F, Nunez J, Kerrigan J, McKenney D, Osborne C, Yu D, Lanieri L, Bojkovic J, Dzink-Fox J, Lilly MD, Sprague ER, Lu Y, Wang H, Ranjitkar S, Xie L, Wang B, Glick M, Hamann LG, Tommasi R, Yang X, Dean CR. Design, synthesis, and properties of a potent inhibitor of *Pseudomonas aeruginosa* deacetylase LpxC. *J Med Chem.* 2017 Jun 22;60(12):5002-5014.
48. Cole KE, Gattis SG, Angell HD, Fierke CA, Christianson DW. Structure of the metal-

- dependent deacetylase LpxC from *Yersinia enterocolitica* complexed with the potent inhibitor CHIR-090. *Biochemistry*. 2011 Jan 18;50(2):258-65.
49. Butler KV, Kalin J, Brochier C, Vistoli G, Langley B, Kozikowski AP. Rational design and simple chemistry yield a superior, neuroprotective HDAC6 inhibitor, tubastatin A. *J Am Chem Soc*. 2010 Aug 11;132(31):10842-6.
50. Wang D. Computational studies on the histone deacetylases and the design of selective histone deacetylase inhibitors. *Curr Top Med Chem*. 2009;9(3):241-56.
51. Chen YD, Jiang YJ, Zhou JW, Yu QS, You QD. Identification of ligand features essential for HDACs inhibitors by pharmacophore modeling. *J Mol Graph Model*. 2008 Apr;26(7):1160-8.
52. Price S, Bordogna W, Bull RJ, Clark DE, Crackett PH, Dyke HJ, Gill M, Harris NV, Gorski J, Lloyd J, Lockey PM, Mullett J, Roach AG, Roussel F, White AB. Identification and optimisation of a series of substituted 5-(1H-pyrazol-3-yl)-thiophene-2-hydroxamic acids as potent histone deacetylase (HDAC) inhibitors. *Bioorg Med Chem Lett*. 2007 Jan 15;17(2):370-5.
53. Tang H, Wang XS, Huang XP, Roth BL, Butler KV, Kozikowski AP, Jung M, Tropsha A. Novel inhibitors of human histone deacetylase (HDAC) identified by QSAR modeling of known inhibitors, virtual screening, and experimental validation. *J Chem Inf Model*. 2009 Feb;49(2):461-76.
54. Park H, Kim S, Kim YE, Lim SJ. A structure-based virtual screening approach toward the discovery of histone deacetylase inhibitors: identification of promising zinc-chelating groups. *ChemMedChem*. 2010 Apr 6;5(4):591-7.
55. Klebe G. *Wirkstoffdesign: Entwurf und Wirkung von Arzneistoffen*. Spektrum Akademischer Verlag 2nd ed, 2009.
56. Molecular Operating Environment (MOE), 2012.10; Chemical Computing Group Inc., 1010 Sherbooke St. West, Suite #910, Montreal, QC, Canada, H3A 2R7, 2012.
57. The PyMOL Molecular Graphics System, Version 2.0 Schrödinger, LLC.
58. Pettersen EF, Goddard TD, Huang CC, Couch GS, Greenblatt DM, Meng EC, Ferrin TE. UCSF Chimera - a visualization system for exploratory research and analysis, *J. Comput. Chem*. 25 (October (13)) (2004) 1605–1612.
59. The UniProt Consortium. Activities at the Universal Protein Resource (UniProt). *Nucleic Acids Res*. 2014 Jan; 42(Database issue): D191–D198.
60. Benson DA, Cavanaugh M, Clark K, Karsch-Mizrachi I, Lipman DJ, Ostell J, Sayers EW. GenBank. *Nucleic Acids Res*. 2013 Jan;41(Database issue):D36-42.
61. Zerlotini A, Aguiar ER, Yu F, Xu H, Li Y, Young ND, Gasser RB, Protasio AV, Berriman

- M, Roos DS, Kissinger JC, Oliveira G. SchistoDB: an updated genome resource for the three key schistosomes of humans. *Nucleic Acids Res.* 2013 Jan;41(Database issue):D728-31.
62. Logan-Klumpler FJ, De Silva N, Boehme U, Rogers MB, Velarde G, McQuillan JA, Carver T, Aslett M, Olsen C, Subramanian S, Phan I, Farris C, Mitra S, Ramasamy G, Wang H, Tivey A, Jackson A, Houston R, Parkhill J, Holden M, Harb OS, Brunk BP, Myler PJ, Roos D, Carrington M, Smith DF, Hertz-Fowler C, Berriman M. GeneDB--an annotation database for pathogens. *Nucleic Acids Res.* 2012 Jan;40(Database issue):D98-108.
63. Berman HM, Westbrook J, Feng Z, Gilliland G, Bhat TN, Weissig H, Shindyalov IN, Bourne PE. The Protein Data Bank. *Nucleic Acids Res.* 2000 Jan 1;28(1):235-42.
64. Altschul SF, Gish W, Miller W, Myers EW, Lipman DJ. Basic local alignment search tool. *J Mol Biol.* 1990, 215, 403-10.
65. Sievers F, Wilm A, Dineen D, Gibson TJ, Karplus K, Li W, Lopez R, McWilliam H, Remmert M, Söding J, Thompson JD, Higgins DG. Fast, scalable generation of high-quality protein multiple sequence alignments using Clustal Omega. *Mol Syst Biol.* 2011 Oct 11;7:539.
66. Eswar N et al. Comparative protein structure modeling using MODELLER. *Current Protocols in Bioinformatics*, John Wiley & Sons, Inc., Supplement 15, 5.6.1-5.6.30, 2006.
67. Shen MY, Sali A. Statistical potential for assessment and prediction of protein structures. *Protein Sci.* 2006 Nov;15(11):2507-24.
68. Robert X, Gouet P. Deciphering key features in protein structures with the new ENDscript server. *Nucleic Acids Res.* 2014 Jul;42(Web Server issue):W320-4.
69. Schrödinger Small-Molecule Drug Discovery Suite 2012: Maestro version 9.3, Protein Preparation Wizard, Epik version 2.3, Glide version 5.8, Schrödinger, LLC, New York, NY, 2012.
70. Banks JL, Beard HS, Cao Y, Cho AE, Damm W, Farid R, Felts AK, Halgren TA, Mainz DT, Maple JR, Murphy R, Philipp DM, Repasky MP, Zhang LY, Berne BJ, Friesner RA, Gallicchio E, Levy RM. Integrated Modeling Program, Applied Chemical Theory (IMPACT). *J Comput Chem.* 2005 Dec;26(16):1752-80.
71. Jones G, Willett P, Glen RC, Leach AR, Taylor R. Development and validation of a genetic algorithm for flexible docking. *J Mol Biol* 1997;267:727-48.
72. Case DA, Darden TA, Cheatham TE III, Simmerling CL, Wang J, Duke RE, Luo R, Walker RC, Zhang W, Merz KM, Roberts B, Hayik S, Roitberg A, Seabra G, Swails J, Götz AW, Kolossváry I, Wong KF, Paesani F, Vanicek J, Wolf RM, Liu J, Wu X, Brozell SR,

- Steinbrecher T, Gohlke H, Cai Q, Ye X, Wang J, Hsieh M-J, Cui G, Roe DR, Mathews DH, Seetin MG, Salomon-Ferrer R, Sagui C, Babin V, Luchko T, Gusarov S, Kovalenko A, and Kollman PA (2012), AMBER 12, University of California, San Francisco.
73. Hornak V, Abel R, Okur A, Strockbine B, Roitberg A, Simmerling C. Comparison of multiple Amber force fields and development of improved protein backbone parameters. *Proteins*. 2006 Nov 15;65(3):712-25.
74. Wang J, Wolf RM, Caldwell JW, Kollman PA, Case DA. Development and testing of a general Amber force field. *J Comput Chem*. 2004 Jul 15;25(9):1157-74.
75. Hoops SC, Anderson KW, Merz KM Jr. Force field design for metalloproteins. *J. Am. Chem. Soc.*, 1991;113(22):8262–70.
76. Jorgensen WL, Chandrasekhar J, Madura JD, Impey RW, Klein ML. Comparison of simple potential functions for simulating liquid water. *J. Chem. Phys.* 1983;79(1):926-935.
77. Darden T, York D, Pedersen L. Particle mesh Ewald: An  $N \cdot \log(N)$  method for Ewald sums in large systems. *J. Chem. Phys.* 1993;98(12):10089-92.
78. Ryckaert J-P, Ciccotti G, Berendsen HJC. Numerical integration of the Cartesian equations of motion of a system with constraints: molecular dynamics of *n*-alkanes. *Journal of Computational Physics* 1977;23(3):327–341.
79. Halgren TA, Merck molecular force field. I. Basis, form, scope, parameterization, and performance of MMFF94. *J. Comput. Chem.*, 17, 490-519 (1996).
80. Gerber PR, Müller K. MAB, a generally applicable molecular force field for structure modelling in medicinal chemistry. *J Comput Aided Mol Des*. 1995 Jun;9(3):251-68.
81. Irwin JJ, Sterling T, Mysinger MM, Bolstad ES, Coleman RG. ZINC: a free tool to discover chemistry for biology. *J Chem Inf Model*. 2012 Jul 23;52(7):1757-68.



## 7. List of Figures

<b>Figure 1.</b> Crystal structure of human HDAC8 with the inhibitor vorinostat (PDB ID 1T69) representing the common architecture of HDAC deacetylase domain.....	6
<b>Figure 2.</b> Putative catalytic mechanism steps (a-d) of the deacetylation reaction in HDAC6.....	7
<b>Figure 3.</b> Crystal structure of <i>E. coli</i> LpxC with the inhibitor LPC-009 (PDB ID 3P3G) representing the common architecture of LpxC fold.....	10
<b>Figure 4.</b> Putative catalytic mechanism steps (a-b) of the deacetylation reaction by <i>E. coli</i> LpxC. .	11
<b>Figure 5.</b> Representative structures of HDAC and LpxC inhibitors.....	12
<b>Figure 6.</b> Shapes and binding modes of HDAC (a-c) and LpxC (d) inhibitors: a) I-shaped broad spectrum HDAC inhibitor vorinostat occupying the substrate binding channel in HDAC2 (PDB ID 4LXZ), b) J-shaped HDAC1-2 selective HDAC inhibitor 20Y targeting the foot pocket in HDAC2 (PDB ID 4LY1), c) L-shaped class IIa selective HDAC inhibitor 9F4 addressing the lower pocket in HDAC4 (PDB ID 4CBT), d) LpxC inhibitor CHIR-090 in <i>Y. enterocolitica</i> LpxC (PDB ID 3NZK) placed in the substrate binding channel.....	14
<b>Figure 7.</b> Novel SmHDAC8 inhibitors identified with a structure-based virtual screening approach (a) and J1038 binding mode (PDB ID 4BZ8) (b).....	37
<b>Figure 8.</b> Optimized SmHDAC8 inhibitors designed using computer-based methods (a) and binding mode of compound 1 (PDB ID 5FUE) (b).....	38

## 8. List of Abbreviations

DOPE	Discrete Optimized Protein Energy
EC	Enzyme Commission number
GAFF	general AMBER force field
GBSA	generalized Born and accessible surface area implicit solvation
HDAC	histone deacetylase
LpxC	UDP-3-O-(R-3-hydroxymyristoyl)-N-acetylglucosamine deacetylase
MD	molecular dynamics
MM	molecular mechanics
QSAR	quantitative structure-activity relationship
RCSB PDB	Research Collaboratory for Structural Bioinformatics Protein Data Bank
RMSD	root-mean-square deviation
SmHDAC8	<i>Schistosoma mansoni</i> histone deacetylase 8
SMILES	simplified molecular-input line-entry system
SP	standard precision
ZBG	zinc-binding group
ZMAL	Z(Ac)Lys-AMC
ZMTFAL	Z(Tfa)Lys-AMC

# 9. Appendix

## 9.1. List of Zinc-Dependent Enzymes

This list is retrieved from ExPASy - ENZYME database in June 2017 and enhanced from the literature. Targets investigated in the current work (HDAC and LpxC) are highlighted in bold font.

### 1. Oxidoreductases

#### 1.1. Acting on the CH-OH group of donors

##### 1.1.1. With NAD(+) or NADP(+) as acceptor

- 1.1.1.1 Alcohol dehydrogenase
- 1.1.1.2 Alcohol dehydrogenase (NADP(+))
- 1.1.1.251 Galactitol-1-phosphate 5-dehydrogenase
- 1.1.1.261 sn-glycerol-1-phosphate dehydrogenase
- 1.1.1.264 L-idonate 5-dehydrogenase (NAD(P)(+))
- 1.1.1.306 S-(hydroxymethyl)mycothiol dehydrogenase
- 1.1.1.324 8-hydroxygeraniol dehydrogenase
- 1.1.1.327 5-exo-hydroxycamphor dehydrogenase
- 1.1.1.329 2-deoxy-scylo-inosamine dehydrogenase
- 1.1.1.360 Glucose/galactose 1-dehydrogenase
- 1.1.1.405 Ribitol-5-phosphate 2-dehydrogenase (NADP(+))

##### 1.1.99. With other acceptors

- 1.1.99.6 D-lactate dehydrogenase (acceptor)
- 1.1.99.36 Alcohol dehydrogenase (nicotinoprotein)
- 1.1.99.37 Methanol dehydrogenase (nicotinoprotein)

#### 1.2. Acting on the aldehyde or oxo group of donors

##### 1.2.7. With an iron-sulfur protein as acceptor

- 1.2.7.4 Anaerobic carbon-monoxide dehydrogenase

##### 1.2.98. With other, known, acceptors

- 1.2.98.1 Formaldehyde dismutase

#### 1.3. Acting on the CH-CH group of donors

##### 1.3.1. With NAD(+) or NADP(+) as acceptor

- 1.3.1.84 Acrylyl-CoA reductase (NADPH)

#### 1.5. Acting on the CH-NH group of donors

##### 1.5.7. With an iron-sulfur protein as acceptor

- 1.5.7.1 Methylenetetrahydrofolate reductase (ferredoxin)

#### 1.6. Acting on NADH or NADPH

##### 1.6.5. With a quinone or similar compound as acceptor

- 1.6.5.5 NADPH:quinone reductase

#### 1.8. Acting on a sulfur group of donors

- 1.8.4. With a disulfide as acceptor
  - 1.8.4.12 Peptide-methionine (R)-S-oxide reductase
- 1.10. Acting on diphenols and related substances as donors
  - 1.10.5. With a quinone or related compound as acceptor
    - 1.10.5.1 Ribosyldihyronicotinamide dehydrogenase (quinone)
- 1.13. Acting on single donors with incorporation of molecular oxygen (oxygenases). The oxygen incorporated need not be derived from O<sub>2</sub>
  - 1.13.11. With incorporation of two atoms of oxygen
    - 1.13.11.29 Stizolobate synthase
    - 1.13.11.30 Stizolobinate synthase
- 1.15. Acting on superoxide as acceptor
  - 1.15.1. Acting on superoxide as acceptor
    - 1.15.1.1 Superoxide dismutase
- 2. Transferases
  - 2.1. Transferring one-carbon groups
    - 2.1.1. Methyltransferases
      - 2.1.1.5 Betaine--homocysteine S-methyltransferase
      - 2.1.1.12 Methionine S-methyltransferase
      - 2.1.1.13 Methionine synthase
      - 2.1.1.14 5-methyltetrahydropteroyltriglutamate--homocysteine S-methyltransferase
      - 2.1.1.247 [Methyl-Co(III) methylamine-specific corrinoid protein]:coenzyme M methyltransferase
      - 2.1.1.n11 Methylphosphotriester-DNA--[protein]-cysteine S-methyltransferase
    - 2.1.3. Carboxy- and carbamoyltransferases
      - 2.1.3.1 Methylmalonyl-CoA carboxytransferase
  - 2.3. Acyltransferases
    - 2.3.1. Transferring groups other than amino-acyl groups
      - 2.3.1.247 3-keto-5-aminohexanoate cleavage enzyme
  - 2.5. Transferring alkyl or aryl groups, other than methyl groups
    - 2.5.1. Transferring alkyl or aryl groups, other than methyl groups
      - 2.5.1.58 Protein farnesyltransferase
      - 2.5.1.59 Protein geranylgeranyltransferase type I
  - 2.7. Transferring phosphorus-containing groups
    - 2.7.1. Phosphotransferases with an alcohol group as acceptor
      - 2.7.1.26 Riboflavin kinase
    - 2.7.7. Nucleotidyltransferases
      - 2.7.7.73 Sulfur carrier protein ThiS adenylyltransferase
  - 2.8. Transferring sulfur-containing groups
    - 2.8.1. Sulfurtransferases
      - 2.8.1.2 3-mercaptopyruvate sulfurtransferase
  - 2.10. Transferring molybdenum- or tungsten-containing groups
    - 2.10.1. Molybdenumtransferases or tungstenttransferases with sulfide groups as acceptors

2.10.1.1 Molybdopterin molybdotransferase

### 3. Hydrolases

#### 3.1. Acting on ester bonds

##### 3.1.1. Carboxylic ester hydrolases

3.1.1.96 D-aminoacyl-tRNA deacylase

##### 3.1.3. Phosphoric monoester hydrolases

3.1.3.1 Alkaline phosphatase

##### 3.1.4. Phosphoric diester hydrolases

3.1.4.3 Phospholipase C

3.1.4.54 N-acetylphosphatidylethanolamine-hydrolyzing phospholipase D

3.1.4.55 Phosphoribosyl 1,2-cyclic phosphate phosphodiesterase

3.1.4.56 7,8-dihydroneopterin 2',3'-cyclic phosphate phosphodiesterase

##### 3.1.6. Sulfuric ester hydrolases

3.1.6.19 (R)-specific secondary-alkylsulfatase

##### 3.1.30. Endoribonucleases active with either ribo- or deoxyribonucleic acids and producing 5'-phosphomonoesters

3.1.30.1 *Aspergillus* nuclease S(1)

#### 3.2. Glycosylases

##### 3.2.1. Glycosidases, i.e. enzymes hydrolyzing O- and S-glycosyl compounds

3.2.1.24 alpha-Mannosidase

#### 3.3. Acting on ether bonds

##### 3.3.2. Ether hydrolases

3.3.2.6 Leukotriene-A(4) hydrolase

#### 3.4. Acting on peptide bonds (peptidases)

##### 3.4.11. Aminopeptidases

3.4.11.1 Leucyl aminopeptidase

3.4.11.2 Membrane alanyl aminopeptidase

3.4.11.3 Cystinyl aminopeptidase

3.4.11.4 Tripeptide aminopeptidase

3.4.11.6 Aminopeptidase B

3.4.11.7 Glutamyl aminopeptidase

3.4.11.10 Bacterial leucyl aminopeptidase

3.4.11.14 Cytosol alanyl aminopeptidase

3.4.11.16 Xaa-Trp aminopeptidase

3.4.11.20 Aminopeptidase Ey

3.4.11.24 Aminopeptidase S

##### 3.4.13. Dipeptidases

3.4.13.18 Cytosol nonspecific dipeptidase

3.4.13.19 Membrane dipeptidase

3.4.13.22 D-Ala-D-Ala dipeptidase

##### 3.4.15. Peptidyl-dipeptidases

3.4.15.1 Peptidyl-dipeptidase A (angiotensin converting enzyme)

- 3.4.15.4 Peptidyl-dipeptidase B
- 3.4.15.5 Peptidyl-dipeptidase Dcp
- 3.4.17. Metallocoxoypeptidases
  - 3.4.17.1 Carboxypeptidase A
  - 3.4.17.2 Carboxypeptidase B
  - 3.4.17.3 Lysine carboxypeptidase
  - 3.4.17.8 Muramoylpentapeptide carboxypeptidase
  - 3.4.17.10 Carboxypeptidase E
  - 3.4.17.11 Glutamate carboxypeptidase
  - 3.4.17.12 Carboxypeptidase M
  - 3.4.17.14 Zinc D-Ala-D-Ala carboxypeptidase
  - 3.4.17.15 Carboxypeptidase A2
  - 3.4.17.18 Carboxypeptidase T
  - 3.4.17.19 Carboxypeptidase Taq
  - 3.4.17.20 Carboxypeptidase U
  - 3.4.17.21 Glutamate carboxypeptidase II
  - 3.4.17.22 Metallocoxoypeptidase D
  - 3.4.17.n1 [CysO sulfur-carrier protein]-S-L-cysteine hydrolase
- 3.4.19. Omega peptidases
  - 3.4.19.6 Pyroglutamyl-peptidase II
  - 3.4.19.15 Desampylase
- 3.4.24. Metalloendopeptidases
  - 3.4.24.1 Atrolysin A
  - 3.4.24.3 Microbial collagenase
  - 3.4.24.6 Leucolysin
  - 3.4.24.7 Interstitial collagenase
  - 3.4.24.11 Neprilysin
  - 3.4.24.12 Envelysin
  - 3.4.24.13 IgA-specific metalloendopeptidase
  - 3.4.24.14 Procollagen N-endopeptidase
  - 3.4.24.15 Thimet oligopeptidase
  - 3.4.24.16 Neurolysin
  - 3.4.24.17 Stromelysin 1
  - 3.4.24.18 Meprin A
  - 3.4.24.19 Procollagen C-endopeptidase
  - 3.4.24.21 Astacin
  - 3.4.24.22 Stromelysin 2
  - 3.4.24.23 Matrilysin
  - 3.4.24.24 Gelatinase A
  - 3.4.24.25 Vibriolysin
  - 3.4.24.26 Pseudolysin
  - 3.4.24.27 Thermolysin

3.4.24.28 Bacillolysin  
3.4.24.29 Aureolysin  
3.4.24.30 Coccolysin  
3.4.24.31 Mycolysin  
3.4.24.32 Beta-lytic metalloendopeptidase  
3.4.24.34 Neutrophil collagenase  
3.4.24.35 Gelatinase B  
3.4.24.36 Leishmanolysin  
3.4.24.37 Saccharolysin  
3.4.24.38 Gametolysin  
3.4.24.39 Deuterolysin  
3.4.24.40 Serralysin  
3.4.24.41 Atrolysin B  
3.4.24.42 Atrolysin C  
3.4.24.43 Atroxase  
3.4.24.44 Atrolysin E  
3.4.24.45 Atrolysin F  
3.4.24.46 Adamalysin  
3.4.24.47 Horrilysin  
3.4.24.48 Ruberlysin  
3.4.24.49 Bothropasin  
3.4.24.50 Bothrolysin  
3.4.24.51 Ophiolysin  
3.4.24.52 Trimerelysin I  
3.4.24.53 Trimerelysin II  
3.4.24.54 Mucrolysin  
3.4.24.55 Pitrilysin  
3.4.24.56 Insulysin  
3.4.24.58 Russellysin  
3.4.24.59 Mitochondrial intermediate peptidase  
3.4.24.61 Nardilysin  
3.4.24.63 Meprin B  
3.4.24.64 Mitochondrial processing peptidase  
3.4.24.65 Macrophage elastase  
3.4.24.66 Choriolysin L  
3.4.24.67 Choriolysin H  
3.4.24.68 Tentoxilysin  
3.4.24.69 Bontoxilysin  
3.4.24.70 Oligopeptidase A  
3.4.24.71 Endothelin-converting enzyme 1  
3.4.24.72 Fibrolase  
3.4.24.73 Jararhagin

- 3.4.24.74 Fragilysin
  - 3.4.24.75 Lysostaphin
  - 3.4.24.76 Flavastacin
  - 3.4.24.77 Snapalysin
  - 3.4.24.79 Pappalysin-1
  - 3.4.24.80 Membrane-type matrix metalloproteinase-1
  - 3.4.24.81 ADAM10 endopeptidase
  - 3.4.24.82 ADAMTS-4 endopeptidase
  - 3.4.24.83 Anthrax lethal factor endopeptidase
  - 3.4.24.84 Ste24 endopeptidase
  - 3.4.24.85 S2P endopeptidase
  - 3.4.24.86 ADAM 17 endopeptidase
  - 3.4.24.89 Pro-Pro endopeptidase
- 3.5. Acting on carbon-nitrogen bonds, other than peptide bonds
- 3.5.1. In linear amides
    - 3.5.1.14 N-acyl-aliphatic-L-amino acid amidohydrolase
    - 3.5.1.58 N-benzyloxycarbonylglycine hydrolase
    - 3.5.1.81 N-acyl-D-amino-acid deacylase
    - 3.5.1.82 N-acyl-D-glutamate deacylase
    - 3.5.1.83 N-acyl-D-aspartate deacylase
    - 3.5.1.88 Peptide Deformylase
    - 3.5.1.91 N-substituted formamide deformylase
    - 3.5.1.98 Histone deacetylase (HDAC)**
    - 3.5.1.103 N-acetyl-1-D-myo-inositol-2-amino-2-deoxy-alpha-D-glucopyranoside deacetylase
    - 3.5.1.108 UDP-3-O-acyl-N-acetylglucosamine deacetylase (LpxC)**
    - 3.5.1.114 N-acyl-aromatic-L-amino acid amidohydrolase
  - 3.5.2. In cyclic amides
    - 3.5.2.1 Barbiturase
    - 3.5.2.6 Beta-lactamase
    - 3.5.2.18 Enamidase
  - 3.5.4. In cyclic amidines
    - 3.5.4.4 Adenosine deaminase
    - 3.5.4.5 Cytidine deaminase
    - 3.5.4.32 8-oxoguanine deaminase
    - 3.5.4.33 tRNA(adenine(34)) deaminase
    - 3.5.4.42 N-isopropylammelide isopropylaminohydrolase
    - 3.5.4.43 Hydroxydechloroatrazine ethylaminohydrolase
    - 3.5.4.46 cAMP deaminase
- 3.11. Acting on carbon-phosphorus bonds
- 3.11.1. Acting on carbon-phosphorus bonds
    - 3.11.1.2 Phosphonoacetate hydrolase



## 4. Lyases

### 4.1. Carbon-carbon lyases

#### 4.1.1. Carboxy-lyases

4.1.1.103 Gamma-resorcyate decarboxylase

#### 4.1.2. Aldehyde-lyases

4.1.2.13 Fructose-bisphosphate aldolase

4.1.2.46 Aliphatic (R)-hydroxynitrile lyase

4.1.2.50 6-carboxytetrahydropterin synthase

### 4.2. Carbon-oxygen lyases

#### 4.2.1. Hydro-lyases

4.2.1.1 Carbonic anhydrase

4.2.1.24 Porphobilinogen synthase

#### 4.2.3. Acting on phosphates

4.2.3.108 1,8-cineole synthase

4.2.3.154 Demethyl-4-deoxygadusol synthase

4.2.3.155 2-epi-valiolone synthase

### 4.4. Carbon-sulfur lyases

#### 4.4.1. Carbon-sulfur lyases

4.4.1.23 2-hydroxypropyl-CoM lyase

4.4.1.27 Carbon disulfide lyase

## 5. Isomerases

### 5.3. Intramolecular oxidoreductases

#### 5.3.1. Interconverting aldoses and ketoses

5.3.1.8 Mannose-6-phosphate isomerase (phosphomannose isomerase)

#### 5.3.3. Transposing C=C bonds

5.3.3.12 L-dopachrome isomerase

## 6. Ligases

### 6.4. Forming carbon-carbon bonds

#### 6.4.1. Forming carbon-carbon bonds

6.4.1.1 Pyruvate carboxylase

## 9.2. Full-Text Manuscripts

Full texts of eleven manuscripts presented in the Results and Discussion chapter are given further.



# Curriculum Vitae

## Personal Information

Name Jelena Melesina  
E-mail jelena.melesina@pharmazie.uni-halle.de  
Address Wolfgang Langenbeck Str 4,  
06120 Halle (Saale), Germany  
Phone +49-345-5525045  
Birthdate 20.04.1986  
Birthplace Shcholkine, Soviet Union  
Citizenship Lithuania  
Languages Russian (native), Lithuanian (native),  
English (advanced), German (intermediate)



## Education

11/2013-03/2018 PhD study at the Institute of Pharmacy,  
The Martin Luther University of Halle-Wittenberg, Halle, Germany  
09/2006-06/2011 Pharmacy study (state examination, grade 5.0/5)  
The North Ossetian State Medical Academy, Vladikavkas, Russia  
09/1998-07/2004 Secondary education (grade 10.0/10),  
“Versmes” Gymnasium of Elektrenai, Elektrenai, Lithuania

## Work Experience

09/2017-03/2018 Research assistant at the Institute of Pharmacy  
The Martin Luther University of Halle-Wittenberg, Halle, Germany  
08/2013-01/2016 Research assistant at the Institute of Pharmacy  
The Martin Luther University of Halle-Wittenberg, Halle, Germany  
10/2012-07/2013 Guest researcher (DAAD-Fellowship) at the Institute of Pharmacy,  
The Martin Luther University of Halle-Wittenberg, Halle, Germany  
02/2012-06/2012 Teaching internship in Pharmacology,  
The North Ossetian State Medical Academy, Vladikavkaz, Russia

## Publication List

- 03/2018 Lecointre B, Narozny R, Borrello MT, Senger J, Chakrabarti A, Jung M, Marek M, Romier C, **Melesina J**, Sippl W, Bischoff L, Ganesan A. Isoform-selective HDAC1/6/8 inhibitors with an imidazo-ketopiperazine cap containing stereochemical diversity. *Phil Trans R Soc B*. 20170364 (in press).
- 03/2018 Simoben CV, Robaa D, Chakrabarti A, Schmidtkunz K, Marek M, Lancelot J, Kannan S, **Melesina J**, Shaik TB, Pierce RJ, Romier C, Jung M, Sippl W. A novel class of *Schistosoma mansoni* histone deacetylase 8 (HDAC8) inhibitors identified by structure-based virtual screening and *in vitro* testing. *Molecules*. 2018 Mar 2;23(3). pii: E566.
- 02/2018 King K, Hauser AT, **Melesina J**, Sippl W, Jung M. Carbamates as potential prodrugs and a new warhead for HDAC inhibition. *Molecules*. 2018 Feb 2;23(2). pii: E321.
- 12/2017 Heimbürg T, Kolbinger FR, Zeyen P, Ghazy E, Herp D, Schmidtkunz K, **Melesina J**, Shaik TB, Erdmann F, Schmidt M, Romier C, Robaa D, Witt O, Oehme I, Jung M, Sippl W. Structure-based design and biological characterization of selective histone deacetylase 8 (HDAC8) inhibitors with anti-neuroblastoma activity. *J Med Chem*. 2017 Dec 28;60(24):10188-204.
- 09/2017 Scholte LLS, Mourão MM, Pais FS, **Melesina J**, Robaa D, Volpini AC, Sippl W, Pierce RJ, Oliveira G, Nahum LA. Evolutionary relationships among protein lysine deacetylases of parasites causing neglected diseases. *Infect Genet Evol*. 2017 Sep;53:175-88.
- 08/2017 Stenzel K, Chakrabarti A, **Melesina J**, Hansen FK, Lancelot J, Herkenhöfner S, Lungerich B, Marek M, Romier C, Pierce RJ, Sippl W, Jung M, Kurz T. Isophthalic acid-based HDAC inhibitors as potent inhibitors of HDAC8 from *Schistosoma mansoni*. *Arch Pharm (Weinheim)*, 2017 Aug;350(8).
- 09/2016 Chakrabarti A, **Melesina J**, Kolbinger FR, Oehme I, Senger J, Witt O, Sippl W, Jung M. Targeting histone deacetylase 8 as a therapeutic approach to cancer and neurodegenerative diseases. *Future Med Chem*. 2016 Sep;8(13):1609-34.

- 03/2016 Heimburg T, Chakrabarti A, Lancelot J, Marek M, **Melesina J**, Hauser AT, Shaik TB, Duclaud S, Robaa D, Erdmann F, Schmidt M, Romier C, Pierce RJ, Jung M, Sippl W. Structure-based design and synthesis of novel inhibitors targeting HDAC8 from *Schistosoma mansoni* for the treatment of schistosomiasis. *J Med Chem*. 2016 Mar 24;59(6):2423-35.
- 03/2016 Tangherlini G, Torregrossa T, Agoglitta O, Köhler J, **Melesina J**, Sippl W, Holl R. Synthesis and biological evaluation of enantiomerically pure glyceric acid derivatives as LpxC inhibitors. *Bioorg Med Chem*. 2016 Mar 1;24(5):1032-44.
- 02/2016 Senger J, **Melesina J**, Marek M, Romier C, Oehme I, Witt O, Sippl W, Jung M. Synthesis and biological investigation of oxazole hydroxamates as highly selective histone deacetylase 6 (HDAC6) inhibitors. *J Med Chem*. 2016 Feb 25;59(4):1545-55.
- 12/2015 Wang L, Kofler M, Brosch G, **Melesina J**, Sippl W, Martinez ED, Easmon J. 2-Benzazolyl-4-piperazin-1-ylsulfonylbenzenecarbohydroxamic acids as novel selective histone deacetylase-6 inhibitors with antiproliferative activity. *PLoS One*. 2015 Dec 23;10(12):e0134556.
- 11/2015 **Melesina J**, Robaa D, Pierce RJ, Romier C, Sippl W. Homology modeling of parasite histone deacetylases to guide the structure-based design of selective inhibitors. *J Mol Graph Model*. 2015 Nov;62:342-61.
- 10/2014 Kannan S, **Melesina J**, Hauser AT, Chakrabarti A, Heimburg T, Schmidtkunz K, Walter A, Marek M, Pierce RJ, Romier C, Jung M, Sippl W. Discovery of inhibitors of *Schistosoma mansoni* HDAC8 by combining homology modeling, virtual screening, and *in vitro* validation. *J Chem Inf Model*. 2014 Oct 27;54(10):3005-19.
- 10/2014 Stolfa DA, Marek M, Lancelot J, Hauser AT, Walter A, Leproult E, **Melesina J**, Rumpf T, Wurtz JM, Cavarelli J, Sippl W, Pierce RJ, Romier C, Jung M. Molecular basis for the antiparasitic activity of a mercaptoacetamide derivative that inhibits histone deacetylase 8 (HDAC8) from the human pathogen *Schistosoma mansoni*. *J Mol Biol*. 2014 Oct 9;426(20):3442-53.
- 02/2014 Szermerski M, **Melesina J**, Wichapong K, Löppenber M, Jose J, Sippl W, Holl R. Synthesis, biological evaluation and molecular docking studies of benzyloxyacetohydroxamic acids as LpxC inhibitors. *Bioorg Med Chem*. 2014 Feb 1;22(3):1016-28.



# Declaration of Authorship

## Selbstständigkeitserklärung

Hiermit erkläre ich, dass ich die vorliegende Dissertationsschrift selbständig und ohne fremde Hilfe angefertigt, keine anderen als die angegebenen Quellen und Hilfsmittel benutzt und die aus ihnen wörtlich oder inhaltlich entnommenen Stellen als solche kenntlich gemacht habe. Die Arbeit wurde ausschließlich der Mathematisch-Naturwissenschaftlichen Fakultät der Martin-Luther-Universität Halle-Wittenberg vorgelegt und an keiner anderen Universität oder Hochschule weder im In- und Ausland zur Erlangung des Doktorgrades eingereicht.

Halle (Saale), den 15.03.2018

---

Jelena Melesina